

Detection and Performance Analysis for Non-Coherent DF Relay Networks with Optimized Generalized Differential Modulation

Yuxin Lu, *Student Member, IEEE*, and Wai Ho Mow, *Senior Member, IEEE*

Abstract

This paper studies the detection and performance analysis problems for a relay network with N parallel decode-and-forward (DF) relays. Due to the distributed nature of this network, it is practically very challenging to fulfill the requirement of instantaneous channel state information for coherent detection. To bypass this requirement, we consider the use of non-coherent DF relaying based on a generalized differential modulation (GDM) scheme, in which transmission power allocation over the M -ary phase shift keying symbols is exploited when performing differential encoding. In this paper, a novel detector at the destination of such a non-coherent DF relay network is proposed. It is an accurate approximation of the state-of-the-art detector, called the almost maximum likelihood detector (AMLD), but the detection complexity is considerably reduced from $\mathcal{O}(M^2N)$ to $\mathcal{O}(MN)$. By characterizing the dominant error terms, we derive an accurate approximate symbol error rate (SER) expression. An optimized power allocation scheme for GDM is further designed based on this SER expression. Our simulation demonstrates that the proposed non-coherent scheme can perform close to the coherent counterpart as the block length increases. Additionally, we prove that the diversity order of both the proposed detector and the AMLD is exactly $\lceil N/2 \rceil + 1$. Extensive simulation results further verify the accuracy of our results in various scenarios.

Index Terms

Cooperative diversity, Channel state information, Decode-and-forward, Differential modulation, Performance analysis

This work was supported by the Hong Kong Research Grants Council under the GRF project no. 16207415. Y. Lu and W. H. Mow are with the Department of Electronic and Computer Engineering, the Hong Kong University of Science and Technology, Hong Kong SAR (e-mail: {ylubg, eewhmow}@ust.hk).

I. INTRODUCTION

Relay-assisted communication is an important technique to enhance the transmission reliability and achieve spatial diversity gains in future wireless systems [1], [2]. Its basic idea is to introduce intermediate relay nodes to forward signals from the source to the destination. It is a particularly attractive technique for applications, such as ad hoc sensor networks, in which the use of multiple antennas is restricted by the size and cost limitations of the terminals. Among various relaying protocols, amplify-and-forward (AF) [3] and decode-and-forward (DF) [4] are the most popularly adopted and widely studied. DF relaying is an ongoing research topic and has found many important usages in many newly emerged applications, such as the Internet of Things (IoT), energy harvesting (EH) networks [5], [6], and unmanned aerial vehicle (UAV) assisted communications [7], [8]. The devices in such systems may form a DF relay network to facilitate reliable communications among them, and they may harvest energy from the received radio signals to meet the power-constrained operating condition [9], [10]. Currently, incorporating DF relaying into these new applications involves a number of new challenges, such as low power consumption and high connectivity [11], [12]. It is thus important to investigate such issues on DF relaying in a timely manner so as to offer some insights and potentially facilitate such efforts.

Coherent detection at the destination of a relay network has been widely studied [13]–[18]. It requires the prior knowledge of the instantaneous channel state information (CSI) of some network links. However, to acquire the instantaneous CSI requires insertion of pilot symbols and frequent channel estimations, which may introduce heavy overhead in terms of bandwidth and power consumption. This becomes a critical issue for future wireless systems facing the challenge of massive connectivity [12]. Besides, the error performance is sensitive to CSI estimation errors. To eliminate the need for instantaneous CSI, differential modulation (DM) with non-coherent detection becomes an attractive alternative [19]–[24]. Unlike the widely studied coherent DF relay network, its non-coherent counterpart has received much less attention. Meanwhile, since in the IoT and UAV relay networks the destination may be a complexity- and energy-constrained device (instead of the base station), low-complexity detection schemes are necessary in order to reduce the hardware complexity and power consumption at the destination.

A drawback of non-coherent detection lies in the performance loss as compared to its coherent counterpart. Specifically, it is well-known that there is a 3 dB performance loss in the case of a point-to-point communication channel, and a similar loss exists in both AF and DF relay

networks using the conventional DM [25]. To address this drawback, the generalized differential modulation (GDM) schemes are designed for AF relay networks in [26], [27]. In GDM, a frame of transmitted symbols is divided into several blocks. In each block, the first symbol is called the reference symbol (RS), and the remaining symbols are called the normal symbols (NSs). The RS of the current block is differentially encoded based on that of the previous block, while the NSs are differentially encoded based on the RS of the current block. RSs and NSs are allocated different transmission power, and the performance can be improved by optimizing the associated power allocation scheme. Since both RSs and NSs convey information, the GDM is one of the most promising techniques that have the potential to improve the performance without reducing the transmission rate as compared to the conventional DM [27], [28]. To our best knowledge, it has not yet been considered for the DF relay networks. For the AF relay networks, the power allocation schemes are obtained by maximizing the average output signal-to-noise ratio (SNR) (of the equivalent point-to-point channel), which is equivalent to minimizing the average symbol error rate (SER) [26], [27]. However, this approach may be highly suboptimal for the DF relay networks due to the problem of erroneous relaying.

This paper considers a single-source single-destination network with N parallel DF relays, assuming the availability of the average CSI at the destination. In this context, non-coherent detection at the destination was studied in [25], [29], [30] for the conventional DM¹. Two state-of-the-art detectors, i.e., the almost maximum likelihood detector (AMLD)² and the piecewise linear detector (PLD), were derived for non-coherent binary frequency shift keying (BFSK) in [25], and later for differential binary phase shift keying (DBPSK) in [29]. They were further extended to general M -ary differential PSK (M -DPSK) and differential M -QAM in [30]. The detection complexity of the AMLD is $\mathcal{O}(M^2N)$, while that of the PLD is $\mathcal{O}(MN)$. As shown in [25], [29], [30], the PLD is an accurate approximation of the AMLD. Some relay decoding error scenarios are ignored by the PLD to achieve the complexity reduction. Analytical SER and diversity order analyses were conducted in [25], [29], [30] for the PLD, whereas no SER analysis results were given for the AMLD to our best knowledge. For ease of discussion, Table I summarizes the known performance analysis results in [25], [29], [30]. It can be seen from the

¹Hereafter, DM will be used to refer to the conventional DM as that used in [25].

²The so-called maximum-likelihood detector introduced in [25] and [29] involves some approximations and is not truly optimal. Hence, it is referred to as the almost maximum likelihood detector here.

TABLE I: Known performance analysis results for the PLD in the non-coherent DF relay network with N parallel relays and a direct link

# of relays	Modulation	SER expression	Diversity order d	Reference
$N = 1$	Non-coherent BFSK	Available	$N + 1$ (full diversity)	[25]
	DBPSK			[29]
	M -DPSK			[30]
$N \geq 2$	Non-coherent BFSK	Unavailable	$d = N/2 + 1$ for N even; $N/2 + 1 \leq d \leq (N + 1)/2 + 1$ for N odd (assuming perfect relay-destination links)	[25]
	DBPSK		$d > N/2 + 1$	[29]
	M -DPSK		$N + 1$ (assuming error-free relays)	[30]

table that the SER expressions for the PLD were obtained only for the single relay case but not for the multiple relay case. In addition, for the multiple relay case (when $N \geq 2$) with M -DPSK, the full diversity order result was obtained under the impractical assumption that all relays are error-free. The main challenge is due to the complexity of performance analysis, which grows exponentially with the number N of relays [25]. This paper aims to tackle the challenge and provide more thorough analyses on the SER and the diversity order.

In this paper, we propose a new detector, thoroughly analyze the error performance, and optimize the transmission power allocation for the non-coherent DF relay networks adopting the GDM scheme based on M -PSK. The main contributions are summarized as follows.

- We propose an $\mathcal{O}(MN)$ -complexity detector, called the near maximum likelihood detector (NMLD), by accurately approximating the detection metric of the $\mathcal{O}(M^2N)$ -complexity AMLD. We also clarify the relation between the detection metrics of the proposed NMLD and the PLD. Our simulation results show that the NMLD performs similarly as the AMLD but with a considerably reduced complexity in various relay channel scenarios. For example, when $M = 8$ and $N = 12$, the number of operations saved by the NMLD compared to the AMLD is up to 84.39%.
- We derive a new approximate SER expression that is applicable to any number of relays and for any value of M . Such SER expression has not been developed in the literature, to our best knowledge. Based on this SER expression, we further design an optimized transmission

power allocation scheme for GDM. As verified by simulation, the SER expression is rather accurate and the proposed scheme can perform close to the coherent counterpart as the block length increases. For example, in the single relay case, for a block length of 256 DQPSK symbols at SER 10^{-5} , the performance gap in SNR is within 0.5 dB.

- By analyzing the high-SNR behavior of our SER expression, we study how the number of erroneous relays affects the diversity order, and prove that the diversity order is exactly $\left\lceil \frac{N}{2} \right\rceil + 1$ for both the NMLD and the AMLD. Such diversity order results are novel in that they are applicable to any value of N (and M). Our simulation results demonstrate that the diversity order results are accurate in various relay channel scenarios.

A. Organization and Notation

The rest of this paper is organized as follows. Sections II-IV are for the single relay network. In Section II, we introduce the GDM transmission scheme followed by a brief review of the AMLD and the PLD for DM. In Section III, our NMLD is proposed. The SER analysis for NMLD is presented in Section IV, followed by the design of an optimized power allocation scheme. The proposed NMLD is extended to the multiple relay network in Section V, where its performance analysis is also performed. Our simulation results with discussions are presented in Section VI, followed by conclusions and future work in Section VII.

Notation: $\text{Re}\{\cdot\}$ denotes the real part of a number or an expression. Bold upper and lower case letters denote matrices and vectors, respectively. $\mathbf{1}_n$ and $\mathbf{0}_n$ stand for all-1 and all-0 column vectors of length n , respectively. $\mathbf{a}[i]$ denotes the i -th element of a vector \mathbf{a} . $\text{diag}(\mathbf{a})$ denotes a diagonal matrix whose diagonal entries starting in the upper left corner are a_1, \dots, a_n . a^* denotes the complex conjugate of a . The sum $\sum_a^b(\cdot)$ is 0 if $a > b$. $\lceil \cdot \rceil$ denotes the ceil operator.

II. SYSTEM MODEL AND EXISTING WORKS

The system model of a multiple relay network is shown in Fig. 1, where N parallel relays R_1, \dots, R_N form N parallel branches in addition to the direct source to destination ($S - D$) link. All relays adopt the DF protocol, and are operated in the half-duplex mode. It is assumed that the relays have no CSI knowledge, and the destination only has the average CSI, i.e., the average link SNRs. $\Theta \triangleq \{1, 2, \dots, N\}$ denotes the relay index set. For the $I - J$ link, $(I, J) \in \{(s, d), (s, r_n), (r_n, d)\}$, $n \in \Theta$, $n_{I,J}$ is used to denote the complex additive white Gaussian noise (AWGN) with zero mean and variance $N_{I,J}$, i.e., $n_{I,J} \sim \mathcal{CN}(0, N_{I,J})$, and $h_{I,J}$ denotes the complex fading coefficient

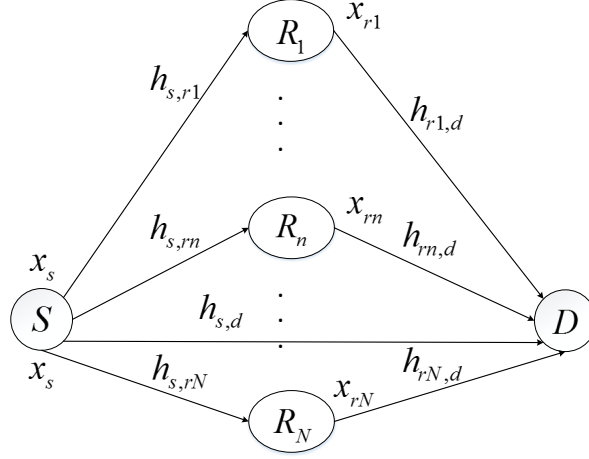


Fig. 1: The system model of a relay network with N parallel relays (R_1, \dots, R_N) and a source to destination ($S - D$) pair.

modeled as a zero-mean complex Gaussian random variable. $\gamma_{I,J} \triangleq \frac{|h_{I,J}|^2}{N_{I,J}}$ is defined as the instantaneous link SNR, and $\bar{\gamma}_{I,J} = \mathbb{E}_{|h_{I,J}|}[\gamma_{I,J}]$ is the average link SNR.

Let the source transmit a frame of K information symbols with an average transmitting power P_s . At symbol time interval $k, k = 1, 2, \dots, K$, the source selects a symbol, denoted as $x_s[k]$, from the M -PSK alphabet, defined as $\mathcal{X} \triangleq \{x_t = e^{j2\pi(t-1)/M}, t = 1, 2, \dots, M\}$, with equal probability. $x_s[k]$ is then differentially encoded as $u_s[k]$ for transmission. Each symbol transmission takes $N + 1$ time slots. In the first time slot, the source broadcasts its differentially encoded signal to all relays and the destination. In the $(n + 1)$ -th time slot, $n \in \Theta$, R_n differentially encodes its detected x_{r_n} for transmission.

A. Generalized Differential Modulation and Transmission

Let us first consider a classical three-node cooperative network, where one relay (R) helps the source (S) to communicate with the destination (D). Fig. 2 shows a diagram of the GDM scheme, in which one frame of $K + 1$ symbols (including the initial symbol $u_s[0]$) is divided into several blocks each with length L . In each block, there are two types of symbols that are allocated different transmission power. The first symbol in each block, denoted as $u_s[bL], b = 0, 1, \dots$, is referred to as the reference symbol (RS) (including the initialization symbol $u_s[0]$), and the other symbols are referred to as the normal symbols (NSs). The RS and NSs are transmitted with the

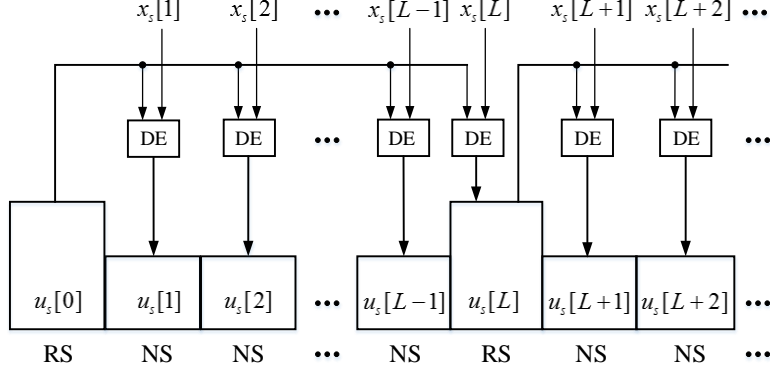


Fig. 2: Diagram of the GDM scheme at the source. Different heights of the blocks denote the different power allocated to the RSs and NSs. Blocks labeled DE represent the differential encoding (DE) operations. A frame of $K+1$ symbols (including the initial symbol $u_s[0]$) is divided into several blocks each with length L .

power values of ρ_T , $T \in \{R, N\}$. The RS in the b -th block is differentially encoded based on the RS in the $(b-1)$ -th block as

$$u_s[bL] = u_s[(b-1)L]x_s[bL], \quad b = 1, 2, \dots, (K+1)/L - 1, \quad (1)$$

where for simplicity, we set $u_s[0] = \sqrt{\rho_R}$, and assume that $(K+1)/L$ is an integer and that ρ_R and ρ_N are known by the receivers, i.e., the relay and destination. The NSs in the b -th block are differentially encoded based on the RS in the same block as

$$u_s[bL + l] = \sqrt{\rho_N/\rho_R} u_s[bL] x_s[bL + l], \quad b = 0, 1, \dots, (K+1)/L - 1, \quad l = 1, 2, \dots, L-1. \quad (2)$$

Based on (1) and (2), the average power constraint at the source should be satisfied as

$$\rho_R + (L-1)\rho_N = LP_s. \quad (3)$$

In the first time slot, the source broadcasts its signal $u_s[k]$, $k = 0, 1, \dots, K$, and the respectively received signals at the relay and the destination are

$$y_{s,J}[k] = h_{s,J}[k]u_s[k] + n_{s,J}[k], \quad J \in \{r, d\}. \quad (4)$$

In the second time slot, the relay performs detection to get $x_r[k]$, differentially encodes $x_r[k]$ as $u_r[k]$ following the same approach as that of the source, and transmits $u_r[k]$ to the destination. Let the relay transmitting power be P_s , and the destination receives

$$y_{r,d}[k] = h_{r,d}[k]u_r[k] + n_{r,d}[k]. \quad (5)$$

For slow Rayleigh fading channels, we follow [26] to assume each $h_{I,J}$, $(I, J) \in \{(s, r), (s, d), (r, d)\}$, remains invariant within one frame duration, while varies independently from one frame to another (quasi-static Rayleigh fading). Then we have for the two consecutive blocks that $h_{I,J}[bL] = h_{I,J}[(b-1)L]$, $b = 1, 2, \dots, (K+1)/L - 1$. Based on (1)-(5), the received signals can be written equivalently as

$$y_{I,J}[bL] = y_{I,J}[(b-1)L]x_I[bL] + n_{I,J}[bL] - x_I[bL]n_{I,J}[(b-1)L], \quad (6)$$

$$y_{I,J}[bL+l] = \sqrt{\rho_N/\rho_R}y_{I,J}[bL]x_I[bL+l] + n_{I,J}[bL+l] - \sqrt{\rho_N/\rho_R}x_I[bL+l]n_{I,J}[bL]. \quad (7)$$

Equations (6) and (7) can be written in a unified form as

$$y_{I,J}[k_1] = \sqrt{\rho_T/\rho_R}y_{I,J}[k_2]x_I[k_1] + n'_{I,J}, \quad (8)$$

where for the RSs, $k_1 = bL$, $k_2 = (b-1)L$ and $T = R$, and for the NSs, $k_1 = bL+l$, $k_2 = bL$ and $T = N$. The noises $n'_{I,J} = n_{I,J}[k_1] - \sqrt{\rho_T/\rho_R}x_I[k_1]n_{I,J}[k_2] \sim \mathcal{CN}(0, (1 + \rho_T/\rho_R)N_{I,J})$.

B. Existing Detectors for the Conventional Differential Modulation

The DM scheme can be regarded as a special case of the GDM scheme when the block length $L = 1$ and all symbols are allocated the same power as $\rho_R = \rho_N = P_s$. For $k = 1, 2, \dots, K$, we have $u_I[k] = u_I[k-1]x_I[k]$ with the power constraint $|u_I[0]|^2 = P_s$, and $y_{I,J}[k] = y_{I,J}[k-1]x_I[k] + n'_{I,J}$ with $n'_{I,J} \sim \mathcal{CN}(0, 2N_{I,J})$, $(I, J) \in \{(s, r), (s, d), (r, d)\}$. The state-of-the-art detectors are the AMLD and the PLD [30]. The optimal maximum likelihood detector for DM is performed as $\max_{x_s \in \mathcal{X}} f(y_{s,d}[k]|x_s, y_{s,d}[k-1]) \sum_{x_r \in \mathcal{X}} \Pr(x_r|x_s) f(y_{r,d}[k]|x_r, y_{r,d}[k-1])$, which finds the transmitted source symbol $x_s \in \mathcal{X}$ that maximizes the conditional joint probability density of the received signals. By approximating the transition probability term $\Pr(x_r|x_s)$ using the average SER at the relay, denoted as ϵ , the AMLD metric is given as

$$f(y_{s,d}[k]|x_s, y_{s,d}[k-1]) \left[(1 - \epsilon) f(y_{r,d}[k]|x_s, y_{r,d}[k-1]) + \frac{\epsilon}{M-1} \sum_{x_r \in \mathcal{X}, x_r \neq x_s} f(y_{r,d}[k]|x_r, y_{r,d}[k-1]) \right]. \quad (9)$$

The AMLD has $\mathcal{O}(M^2)$ complexity. Based on (9), the $\mathcal{O}(M)$ -complexity PLD can be developed by omitting some probability terms and applying the piece-wise linear approximation. The detection metric of the PLD will be discussed in detail in Section V-A, where we analyze the relation between the PLD and the proposed NMLD.

III. SINGLE RELAY DETECTION

In this section, we derive an expression of the average SER at the relay (the value of ϵ) and introduce our $\mathcal{O}(M)$ -complexity near maximum likelihood detector (NMLD).

A. Average SER at the Relay

The optimal detection at the relay can be performed as $x_r[k_1] = \arg \min_{x \in \mathcal{X}} |y_{s,r}[k_1] - \sqrt{\rho_T/\rho_R} y_{s,r}[k_2]x|^2$ according to (8). For the $I - J$ link, by ignoring the higher order noise terms [30], the average receive SNR can be obtained as

$$\mathbb{E}_{|h_{I,J}|} \left[\frac{(\rho_T/\rho_R)|y_{I,J}[k_2]|^2}{(1 + \rho_T/\rho_R)N_{I,J}} \right] \approx \phi_T \bar{\gamma}_{I,J}, \quad T \in \{R, N\}, \quad (10)$$

where $\phi_T \triangleq \frac{1}{1/\rho_T + 1/\rho_R}$. Based on (10), an expression of ϵ can be obtained (see (41) and its derivation in Appendix A).

B. NMLD at the Destination

Based on (8) and (9), the AMLD metric for GDM can be written straightforwardly as

$$\begin{aligned} & f(y_{s,d}[k_1]|x_s, y_{s,d}[k_2]) \left[(1 - \epsilon) f(y_{r,d}[k_1]|x_s, y_{r,d}[k_2]) + \epsilon/(M - 1) \sum_{\substack{x_r \in \mathcal{X} \\ x_r \neq x_s}} f(y_{r,d}[k_1]|x_r, y_{r,d}[k_2]) \right] \\ &= \exp\left(-|y_{s,d}[k_1] - \sqrt{\rho_T/\rho_R} y_{s,d}[k_2]x_s|^2/N_{s,d}\right) \left[(1 - \epsilon) \exp\left(-|y_{r,d}[k_1] - \sqrt{\rho_T/\rho_R} y_{r,d}[k_2]x_s|^2/N_{r,d}\right) \right. \\ & \quad \left. + \epsilon/(M - 1) \sum_{x_r \in \mathcal{X}, x_r \neq x_s} \exp\left(-|y_{r,d}[k_1] - \sqrt{\rho_T/\rho_R} y_{r,d}[k_2]x_r|^2/N_{r,d}\right) \right]. \end{aligned} \quad (11)$$

By applying the widely-used max-sum approximation (see also [16], [31]) to replace the summation operations of the exponentials in (11) with the maximum operations, we obtain the detection rule of the NMLD as

$$\begin{aligned} \hat{x}_s &= \arg \max_{x_s \in \mathcal{X}} \left\{ \exp\left(-|y_{s,d}[k_1] - \sqrt{\rho_T/\rho_R} y_{s,d}[k_2]x_s|^2/N_{s,d}\right) \max\left\{ (1 - \epsilon) \exp\left(-|y_{r,d}[k_1] - \sqrt{\rho_T/\rho_R} y_{r,d}[k_2]x_s|^2/N_{r,d}\right), \right. \right. \\ & \quad \left. \left. \epsilon/(M - 1) \max_{x_r \in \mathcal{X}, x_r \neq x_s} \exp\left(-|y_{r,d}[k_1] - \sqrt{\rho_T/\rho_R} y_{r,d}[k_2]x_r|^2/N_{r,d}\right) \right\} \right\} \\ &= \arg \min_{x_s \in \mathcal{X}} \left\{ \frac{1}{N_{s,d}} |y_{s,d}[k_1] - \sqrt{\rho_T/\rho_R} y_{s,d}[k_2]x_s|^2 + \min\left\{ \frac{1}{N_{r,d}} |y_{r,d}[k_1] - \sqrt{\rho_T/\rho_R} y_{r,d}[k_2]x_s|^2, \right. \right. \\ & \quad \left. \left. \min_{x_r \in \mathcal{X}, x_r \neq x_s} \frac{1}{N_{r,d}} |y_{r,d}[k_1] - \sqrt{\rho_T/\rho_R} y_{r,d}[k_2]x_r|^2 + \eta \right\} \right\} \end{aligned} \quad (12)$$

$$\begin{aligned} &= \arg \min_{x_s \in \mathcal{X}} \left\{ \frac{1}{N_{s,d}} |y_{s,d}[k_1] - \sqrt{\rho_T/\rho_R} y_{s,d}[k_2]x_s|^2 + \min\left\{ \frac{1}{N_{r,d}} |y_{r,d}[k_1] - \sqrt{\rho_T/\rho_R} y_{r,d}[k_2]x_s|^2, \right. \right. \\ & \quad \left. \left. \min_{x_r \in \mathcal{X}} \frac{1}{N_{r,d}} |y_{r,d}[k_1] - \sqrt{\rho_T/\rho_R} y_{r,d}[k_2]x_r|^2 + \eta \right\} \right\}, \end{aligned} \quad (13)$$

where $\eta \triangleq (1 + \rho_T/\rho_R) \log \frac{(1-\epsilon)(M-1)}{\epsilon}$. From (12) to (13), we remove the constraint of $x_r \neq x_s$. This is because $\eta > 0$ holds when $\epsilon < 1/2$ and $M \geq 2$, which is considered to be true. The NMLD with $\mathcal{O}(M)$ complexity can be implemented according to (13), as described next. First, we solve

for $C_1 = \min_{x_r \in \mathcal{X}} \frac{1}{N_{r,d}} |y_{r,d}[k_1] - \sqrt{\rho_T/\rho_R} y_{r,d}[k_2] x_r|^2 + \eta$, and the obtained C_1 value becomes a fixed threshold. This step has complexity $\mathcal{O}(M)$ since $|\mathcal{X}| = M$, where $|\mathcal{X}|$ denotes the cardinality of \mathcal{X} . Then, for each $x_s \in \mathcal{X}$, we compare the value of $\frac{1}{N_{r,d}} |y_{r,d}[k_1] - \sqrt{\rho_T/\rho_R} y_{r,d}[k_2] x_s|^2$ with C_1 , and calculate the detection metrics to choose the symbol x_s with the smallest metric value as \hat{x}_s . This step also has complexity $\mathcal{O}(M)$. Overall, the complexity of the NMLD is $\mathcal{O}(M)$.

IV. SER PERFORMANCE AND OPTIMIZED POWER ALLOCATION SCHEME

In this section, we derive an approximate SER expression, and based on which an optimized power allocation scheme is obtained. The solutions to all optimization problems under consideration will be given in explicit forms.

The overall error probability can be written as $\Pr[\text{error}] = (1 - \epsilon) \Pr[\text{error}|\text{error-free relaying}] + \epsilon \Pr[\text{error}|\text{erroneous relaying}]$. $\Pr[\text{error}|\text{error-free relaying}]$ and $\Pr[\text{error}|\text{erroneous relaying}]$ characterize the conditional SER performances for the scenarios of error-free relaying and erroneous relaying, respectively. Error-free (erroneous) relaying means that the relay detects correctly (wrongly). The key idea is to determine the dominant pairwise error probability (PEP) terms for the above two scenarios. To facilitate later analysis, the following primary results are presented.

For notational convenience, we define $\lambda(t_1, t_2) \triangleq \frac{1}{N_{s,d}} |y_{s,d}[k_1] - \sqrt{\rho_T/\rho_R} y_{s,d}[k_2] t_1|^2 + \frac{1}{N_{r,d}} |y_{r,d}[k_1] - \sqrt{\rho_T/\rho_R} y_{r,d}[k_2] t_2|^2$, and write the detection metric in (12) equivalently as

$$\begin{aligned} & \min \left\{ \min_{x_s \in \mathcal{X}} \lambda(x_s, x_s), \min_{(x_s, x_r) \in \mathcal{X}^2, x_r \neq x_s} \lambda(x_s, x_r) + \eta \right\} \\ &= \min_{x_s \in \mathcal{X}} \min_{x_r \in \mathcal{X}, x_r \neq x_s} \{ \lambda(x_s, x_s), \lambda(x_s, x_r) + \eta \}, \end{aligned}$$

where the detection metric associated with a symbol pair (x_s, x_r) is $\lambda(x_s, x_s)$ if $x_s = x_r$ and is $\lambda(x_s, x_r) + \eta$ otherwise. For performance analysis convenience and without loss of generality, the transmitted symbol pair from the source and the relay is denoted as $(x_1, x_r) \in \mathcal{X}^2$. We consider the case when x_1 is wrongly detected to any other symbol $x_v \in \mathcal{X}$ at the destination, and denote the competing symbol pair as $(x_v, x_u) \in \mathcal{X}^2$, $x_v \neq x_1$.

For $(t_1, t_2) \in \mathcal{X}^2$ and $I \in \{s, r\}$, we define $\omega_{I,d}(t_1, t_2) \triangleq \frac{1}{2\sqrt{\rho_T/\rho_R} N_{I,d}} \left(|y_{I,d}[k_1] - \sqrt{\rho_T/\rho_R} y_{I,d}[k_2] t_1|^2 - |y_{I,d}[k_1] - \sqrt{\rho_T/\rho_R} y_{I,d}[k_2] t_2|^2 \right)$, and $\omega_{I,d}(t_1, t_2)$ denotes the difference between their associated $I-d$ link metrics. Then according to (12), we have

$$\lambda(x_1, x_r) - \lambda(x_v, x_u) = 2\sqrt{\rho_T/\rho_R} (\omega_{s,d}(x_1, x_v) + \omega_{r,d}(x_r, x_u)). \quad (14)$$

By substituting the expressions of $y_{I,d}[k_1]$ and $y_{I,d}[k_2]$ (based on the system equations given in Section II-A) it yields

$$\begin{aligned} \omega_{I,d}(t_1, t_2) = & \frac{1}{N_{I,d}} \text{Re}\{\sqrt{\rho_T \rho_R} |h_{I,d}|^2 x_I^*(t_2 - t_1) + h_{I,d}^* \sqrt{\rho_T / \rho_R} u_I^*[k_2] x_I^*(t_2 - t_1) n_{I,d}[k_2] + \\ & y_{I,d}[k_2] (t_2 - t_1) n_{I,d}^*[k_1]\}, \end{aligned} \quad (15)$$

where $h_{I,d}[k_1] = h_{I,d}[k_2] = h_{I,d}$. Similar to (10), by ignoring the higher order noise terms in (15), it can be shown after some calculations that $\omega_{I,d}(t_1, t_2) \sim \mathcal{N}(u_{I,d}(t_1, t_2), W_{I,d}(t_1, t_2))$ with

$$u_{I,d}(t_1, t_2) = \sqrt{\rho_T \rho_R} \text{Re}\{x_I^*(t_2 - t_1)\} \gamma_{I,d}, \quad (16)$$

$$W_{I,d}(t_1, t_2) = \frac{1}{2} \rho_R (1 + \rho_T / \rho_R) |t_2 - t_1|^2 \gamma_{I,d}. \quad (17)$$

A. SER Performance for Error-Free Relaying

The scenario of error-free relaying happens with probability $1 - \epsilon$, in which we have $(x_1, x_r) = (x_1, x_1)$. The conditional error probability for detecting (x_1, x_1) as (x_v, x_u) can be written as

$$\begin{aligned} & \Pr[\lambda(x_1, x_1) > \min_{x_u \neq x_v} \{\lambda(x_v, x_v), \lambda(x_v, x_u) + \eta\}] \\ &= \Pr[\lambda(x_v, x_v) < \lambda(x_v, x_u) + \eta, \lambda(x_1, x_1) > \lambda(x_v, x_v)] + \\ & \Pr[\lambda(x_v, x_v) > \lambda(x_v, x_u) + \eta, \lambda(x_1, x_1) > \lambda(x_v, x_u) + \eta], \quad x_u \neq x_v \\ &\stackrel{(a)}{=} \Pr[\omega_{r,d}(x_v, x_u) < \frac{\eta}{2\sqrt{\rho_T / \rho_R}}, \omega_{s,d}(x_1, x_v) + \omega_{r,d}(x_1, x_v) > 0] + \\ & \Pr\left[\omega_{r,d}(x_v, x_u) > \frac{\eta}{2\sqrt{\rho_T / \rho_R}}, \omega_{s,d}(x_1, x_v) + \omega_{r,d}(x_1, x_u) > \frac{\eta}{2\sqrt{\rho_T / \rho_R}}\right], \quad x_u \neq x_v, \end{aligned}$$

and upper bounded by

$$\Pr[\omega_{s,d}(x_1, x_v) + \omega_{r,d}(x_1, x_v) > 0] + \Pr\left[\omega_{s,d}(x_1, x_v) + \omega_{r,d}(x_1, x_u) > \frac{\eta}{2\sqrt{\rho_T / \rho_R}}\right], \quad x_u \neq x_v, \quad (18)$$

where (a) is obtained according to (14). We assume that x_1 is wrongly detected to its two nearest neighbors, i.e., $x_v \in \{x_2, x_M\}$, at the destination, which is well justified for the scenario of error-free relaying. Then the problem of obtaining the dominant PEP terms in (18) is formulated as

$$\begin{aligned} \text{(P1)} \quad & \underset{x_v, x_u}{\text{maximize}} \quad \left\{ \Pr[\omega_{s,d}(x_1, x_v) + \omega_{r,d}(x_1, x_v) > 0], \Pr\left[\omega_{s,d}(x_1, x_v) + \omega_{r,d}(x_1, x_u) > \frac{\eta}{2\sqrt{\rho_T / \rho_R}}\right] \right\} \\ & \text{subject to} \quad x_v \in \{x_2, x_M\}, x_u \in \mathcal{X}, x_u \neq x_v. \end{aligned}$$

It can be observed that the exact solution to problem (P1) varies with channel coefficients $h_{s,d}$ and $h_{r,d}$, and our approach is to take all possible solutions and obtain a solution set, considering all values of $h_{s,d}$ and $h_{r,d}$. There are two probability terms in the objective function of (P1), and we subsequently maximize them. For the first term, according to (16) and (17), we ignore the higher order noise and maximize

$$\Pr[\omega_{s,d}(x_1, x_v) + \omega_{r,d}(x_1, x_v) > 0] \approx Q\left(\sqrt{\phi_T \operatorname{Re}\{1 - x_1^* x_v\}(\gamma_{s,d} + \gamma_{r,d})}\right). \quad (19)$$

This is equivalent to minimize $\operatorname{Re}\{1 - x_1^* x_v\}$, of which the solutions are obtained when $x_v \in \{x_2, x_M\}$.

For the second term, similarly, we maximize

$$\begin{aligned} & \Pr\left[\omega_{s,d}(x_1, x_v) + \omega_{r,d}(x_1, x_u) > \frac{\eta}{2\sqrt{\rho_T/\rho_R}}\right] \\ & \approx Q\left(\frac{\frac{\eta}{2\sqrt{\rho_T/\rho_R}} - \sqrt{\rho_T\rho_R}(\operatorname{Re}\{x_1^*(x_v - x_1)\}\gamma_{s,d} + \operatorname{Re}\{x_1^*(x_u - x_1)\}\gamma_{r,d})}{\sqrt{\frac{1}{2}\rho_R(1 + \rho_T/\rho_R)(|x_v - x_1|^2\gamma_{s,d} + |x_u - x_1|^2\gamma_{r,d})}}\right). \end{aligned} \quad (20)$$

It is observed that only when $x_u = x_1$, the value of (20) could be larger than that of (19) with $x_v \in \{x_2, x_M\}$. Then the solutions for maximizing the second term are obtained when $x_v \in \{x_2, x_M\}, x_u = x_1$.

Overall, the solution set to problem (P1) is obtained when $(x_v, x_u) \in \{(x_2, x_2), (x_M, x_M), (x_2, x_1), (x_M, x_1)\}$. By summing over all elements in the solution set based on (19) and (20), an approximate SER expression can be obtained as

$$\begin{aligned} & (1 - \epsilon) \sum_{(x_v, x_u) \in \{(x_2, x_2), (x_M, x_M)\}} \Pr[\omega_{s,d}(x_1, x_v) + \omega_{r,d}(x_1, x_v) > 0] + \\ & (1 - \epsilon) \sum_{(x_v, x_u) \in \{(x_2, x_1), (x_M, x_1)\}} \Pr\left[\omega_{s,d}(x_1, x_v) + \omega_{r,d}(x_1, x_u) > \frac{\eta}{2\sqrt{\rho_T/\rho_R}}\right] \\ & \approx 2(1 - \epsilon)Q\left(\sin\left(\frac{\pi}{M}\right)\sqrt{2\phi_T(\gamma_{s,d} + \gamma_{r,d})}\right) + \\ & 2(1 - \epsilon)Q\left(\sin\left(\frac{\pi}{M}\right)\sqrt{2\phi_T\gamma_{s,d}} + \frac{\eta}{2(1 + \rho_T/\rho_R)\sin\left(\frac{\pi}{M}\right)\sqrt{2\phi_T\gamma_{s,d}}}\right), \quad T \in \{R, N\}. \end{aligned} \quad (21)$$

B. SER Performance for Erroneous Relaying

The scenario of erroneous relaying happens with probability ϵ , in which we have $x_r \neq x_1$. The conditional error probability for detecting (x_1, x_r) as (x_v, x_u) can be written as

$$\begin{aligned}
& \Pr [\lambda(x_1, x_r) + \eta > \min_{x_u \neq x_v} \{\lambda(x_v, x_v), \lambda(x_v, x_u) + \eta\}] \\
&= \Pr[\lambda(x_v, x_v) > \lambda(x_v, x_u) + \eta, \lambda(x_1, x_r) + \eta > \lambda(x_v, x_u) + \eta] + \\
& \quad \Pr[\lambda(x_v, x_v) < \lambda(x_v, x_u) + \eta, \lambda(x_1, x_r) + \eta > \lambda(x_v, x_v)], \quad x_u \neq x_v \\
&\stackrel{(b)}{=} \Pr \left[\omega_{r,d}(x_v, x_u) > \frac{\eta}{2\sqrt{\rho_T/\rho_R}}, \omega_{s,d}(x_1, x_v) + \omega_{r,d}(x_r, x_u) > 0 \right] + \\
& \quad \Pr \left[\omega_{r,d}(x_v, x_u) < \frac{\eta}{2\sqrt{\rho_T/\rho_R}}, \omega_{s,d}(x_1, x_v) + \omega_{r,d}(x_r, x_v) > -\frac{\eta}{2\sqrt{\rho_T/\rho_R}} \right], \quad x_u \neq x_v,
\end{aligned}$$

and upper bounded by

$$\Pr[\omega_{s,d}(x_1, x_v) + \omega_{r,d}(x_r, x_u) > 0] + \Pr \left[\omega_{s,d}(x_1, x_v) + \omega_{r,d}(x_r, x_v) > -\frac{\eta}{2\sqrt{\rho_T/\rho_R}} \right], \quad x_u \neq x_v, \quad (22)$$

where (b) is obtained according to (14). The dominant terms in (22) can be found by solving the two problems (P2.1) and (P2.2) as

$$\begin{aligned}
\text{(P2.1)} \quad & \underset{x_v, x_u}{\text{maximize}} \quad \Pr[\omega_{s,d}(x_1, x_v) + \omega_{r,d}(x_r, x_u) > 0] \\
& \text{subject to} \quad (x_v, x_u) \in \mathcal{X}^2, x_v \neq x_1, x_u \neq x_v.
\end{aligned}$$

$$\begin{aligned}
\text{(P2.2)} \quad & \underset{x_v}{\text{maximize}} \quad \Pr \left[\omega_{s,d}(x_1, x_v) + \omega_{r,d}(x_r, x_v) > -\frac{\eta}{2\sqrt{\rho_T/\rho_R}} \right] \\
& \text{subject to} \quad x_v \in \mathcal{X}, x_v \neq x_1.
\end{aligned}$$

Different from problem (P1) in the scenario of error-free relaying, we formulate the two separate problems (P2.1) and (P2.2) to include more dominant terms. This is in consideration of the accuracy of the SER expression at low SNRs. For problem (P2.1), according to (16) and (17), we have

$$\Pr[\omega_{s,d}(x_1, x_v) + \omega_{r,d}(x_r, x_u) > 0] \approx Q \left(\frac{-\sqrt{\rho_T \rho_R} (\gamma_{s,d} \text{Re}\{x_1^*(x_v - x_1)\} + \gamma_{r,d} \text{Re}\{x_r^*(x_u - x_r)\})}{\sqrt{\frac{1}{2} \rho_R (1 + \rho_T/\rho_R) (\gamma_{s,d} |x_v - x_1|^2 + \gamma_{r,d} |x_u - x_r|^2)}} \right). \quad (23)$$

Based on (23), we have that problem (P2.1) can be written as $\underset{x_u, x_v}{\text{minimize}} \gamma_{s,d} \text{Re}\{1 - x_1^* x_v\} + \gamma_{r,d} \text{Re}\{1 - x_r^* x_u\}$, of which the solutions are obtained when $x_v \in \{x_2, x_M\}, x_u = x_r$. Similarly for problem (P2.2), the objective function becomes

$$Q \left(\frac{-\frac{\eta}{2\sqrt{\rho_T/\rho_R}} - \sqrt{\rho_T \rho_R} (\gamma_{s,d} \text{Re}\{x_1^*(x_v - x_1)\} + \gamma_{r,d} \text{Re}\{x_r^*(x_v - x_r)\})}{\sqrt{\frac{1}{2} \rho_R (1 + \rho_T/\rho_R) (\gamma_{s,d} |x_v - x_1|^2 + \gamma_{r,d} |x_v - x_r|^2)}} \right). \quad (24)$$

It is straightforward to prove that the right side of (24) is monotonically decreasing in the term $\gamma_{s,d} \text{Re}\{1 - x_1^* x_v\} + \gamma_{r,d} \text{Re}\{1 - x_r^* x_v\}$, provided that the values of $\text{Re}\{1 - x_1^* x_v\}$ and $\text{Re}\{1 - x_r^* x_v\}$ are both non-negative, which holds true for M -DPSK. Therefore problem (P2.2) can be written as $\underset{x_v}{\text{minimize}} \gamma_{s,d} \text{Re}\{1 - x_1^* x_v\} + \gamma_{r,d} \text{Re}\{1 - x_r^* x_v\}$. To tighten the SER expression, x_r is included as an additional optimization variable, and the objective becomes $\underset{x_v, x_r}{\text{minimize}} \gamma_{s,d} \text{Re}\{1 - x_1^* x_v\} + \gamma_{r,d} \text{Re}\{1 - x_r^* x_v\}$ (with added constraints $x_r \in \mathcal{X}$, $x_r \neq x_1$), and then the solutions are obtained when $x_v = x_r \in \{x_2, x_M\}$.

Overall, the solution sets to problems (P2.1) and (P2.2) are obtained when $(x_v, x_u) \in \{(x_2, x_r), (x_M, x_r)\}$ and $x_v = x_r \in \{x_2, x_M\}$, respectively. By summing over all elements in the solution sets based on (23) and (24), an SER expression is obtained as

$$\begin{aligned} & \frac{\epsilon}{M-1} \sum_{(x_v, x_u) \in \{(x_2, x_r), (x_M, x_r)\}} \Pr[\omega_{s,d}(x_1, x_v) + \omega_{r,d}(x_r, x_u) > 0] + \\ & \frac{\epsilon}{M-1} \sum_{x_v = x_r \in \{x_2, x_M\}} \Pr \left[\omega_{s,d}(x_1, x_v) + \omega_{r,d}(x_r, x_v) > -\frac{\eta}{2\sqrt{\rho_T/\rho_R}} \right] \\ & \approx 2\epsilon Q \left(\sin\left(\frac{\pi}{M}\right) \sqrt{2\phi_T \gamma_{s,d}} \right) + \\ & \frac{2\epsilon}{M-1} Q \left(\sin\left(\frac{\pi}{M}\right) \sqrt{2\phi_T \gamma_{s,d}} - \frac{\eta}{2(1 + \rho_T/\rho_R) \sin(\frac{\pi}{M}) \sqrt{2\phi_T \gamma_{s,d}}} \right), \quad T \in \{R, N\}. \end{aligned} \quad (25)$$

Finally, (25) together with (21) constitute the overall SER expression. Note that for $M = 2$ (the BPSK case), the terms $2(1 - \epsilon)$ in (21) and 2ϵ in (25) should be replaced by $(1 - \epsilon)$ and ϵ , respectively. For Rayleigh fading channels, the average SER can be calculated by averaging over the channel coefficients $h_{s,d}$ and $h_{r,d}$. The expression will be derived in Section V.

C. Optimized Power Allocation Scheme

As shown in (10), the average receive SNR $\phi_T \bar{\gamma}_{I,J}$, $(I, J) \in \{(s, d), (s, r), (r, d)\}$, is proportional to ϕ_T . Therefore, in the scenario of error-free relaying, maximizing ϕ_T is equivalent to minimizing the SER. Next, we optimize the SER performance for the scenario of erroneous relaying, by minimizing the SER expression given in (25). To show the advantages of GDM, the NSs usually take more portion than the RSs [26], [27], i.e., $L \gg 1$. Therefore we focus on the NSs with $T = N$, and then we have $\phi_N = \frac{1}{1/\rho_N + 1/\rho_R}$.

There are two summation terms in (25), and we analyze their monotonicity properties with respect to ϕ_N subsequently. It is straightforward to show that ϵ is monotonically decreasing with ϕ_N by taking derivative, and we have that the first term in (25) is monotonically decreasing

in ϕ_N . We prove in Appendix B that the second term is also monotonically decreasing in ϕ_N , provided that the condition $(\rho_R, \rho_N) \in \mathbb{S}$ is satisfied, with

$$\mathbb{S} = \left\{ (\rho_R, \rho_N) \middle| \phi_N = \frac{1}{1/\rho_N + 1/\rho_R}, \frac{\log \frac{(1-\epsilon)(M-1)}{\epsilon}}{4 \sin^2(\frac{\pi}{M}) \phi_N \gamma_{s,d}} \rightarrow \infty \right\}. \quad (26)$$

In this context, both summation terms in (25) are monotonically decreasing in ϕ_N , and minimizing (25) can be achieved by maximizing ϕ_N .

Finally, the objective becomes maximizing $\phi_N = \frac{1}{1/\rho_N + 1/\rho_R}$, and the problem is formulated as

$$\begin{aligned} & \underset{\rho_R, \rho_N}{\text{maximize}} && \frac{1}{1/\rho_N + 1/\rho_R} \\ & \text{subject to} && \rho_R + (L-1)\rho_N = LP_s, \end{aligned} \quad (27a)$$

(P3)

$$\rho_N > 0, \rho_R > 0, \quad (27b)$$

$$(\rho_R, \rho_N) \in \mathbb{S}, \quad (27c)$$

where (27a) is due to the average power constraint at the source (given in (3)). The constraint of (27c) is too complicated to be addressed directly, considering that both ϕ_N and ϵ are functions of ρ_R and ρ_N (see (26) and (41)). As an alternative, we first ignore (27c) to obtain a solution, and then verify (27c) by substituting the solution. Without constraint (27c), problem (P3) degrades to that in [26, eq. (25)] for AF relaying. It can be solved in several ways, such as using the Lagrange multiplier method, and the solution is obtained as

$$(\rho_R^*, \rho_N^*) = \left(\frac{LP_s}{1 + \sqrt{L-1}}, \frac{LP_s}{L-1 + \sqrt{L-1}} \right). \quad (28)$$

By substituting (28) into (27c) it yields the condition that $\frac{\log \frac{(1-\epsilon^*)(M-1)}{\epsilon^*}}{2z_{L,M}^2 \gamma_{s,d}} \rightarrow \infty$ with $z_{L,M} = \sin(\frac{\pi}{M}) \sqrt{\frac{2LP_s}{L+2\sqrt{L-1}}}$, and ϵ^* is calculated from (41) using $(\rho_R, \rho_N) = (\rho_R^*, \rho_N^*)$. To gain a better understanding of this condition, we give an interpretation in terms of the SNRs of the $S-D$ and $S-R$ links. Since $1/2 \leq \frac{L}{L+2\sqrt{L-1}} < 1$ when $L \geq 2$, $z_{L,M}$ is guaranteed to be a bounded positive value for all $M > 1$. In addition, since ϵ denotes the average SER of the $S-R$ link, we have $\frac{1}{\epsilon^*} \propto \bar{\gamma}_{s,r}$. Based on the above, we have $\frac{\log \frac{(1-\epsilon^*)(M-1)}{\epsilon^*}}{2z_{L,M}^2 \gamma_{s,d}} \rightarrow \infty \iff \frac{\log \frac{(1-\epsilon^*)}{\epsilon^*}}{\gamma_{s,d}} \rightarrow \infty \iff \frac{\log \bar{\gamma}_{s,r}}{\gamma_{s,d}} \rightarrow \infty$. It is now clear that the condition can be satisfied when the average SNR of the $S-R$ link $\bar{\gamma}_{s,r}$ is much larger than the instantaneous SNR of the $S-D$ link $\gamma_{s,d}$. This is generally practical for the DF relay network, in which the help from a relatively strong $S-R$ link is needed usually because the direct $S-D$ link is relatively weak.

Let us focus on the solution in (28) and get insights on how this optimized power allocation scheme works. We first note that only the values of P_s and L are needed to obtain ρ_R^* and ρ_N^* ,

while no prior information of the channels are required. $\rho_R^*/\rho_N^* = \sqrt{L-1}$ only depends on the block length L . For $L = 2$, we have $\rho_R^* = \rho_N^* = P_s$, which means all symbols are allocated the same power as P_s . For $L > 2$, we have $\rho_R^*/\rho_N^* > 1$, which reveals that to show the advantages of GDM, more power should be allocated to the RSs. It is obvious that the value of L largely affects the performance of the optimized power allocation scheme, and this effect will be discussed by simulation in Section VI.

V. MULTIPLE RELAY DETECTION AND PERFORMANCE ANALYSIS

A. Multiple Relay Detection

Let us recall that the multi-relay system model has been stated in Section II. The GDM scheme is applied, and each relay processes and transmits symbols as R does in the single relay case. At the destination, the optimal maximum likelihood detection metric is given as $\max_{x_s \in \mathcal{X}} f(y_{s,d}[k_1]|x_s, y_{s,d}[k_2]) \prod_{n \in \Theta} \left(\sum_{x_{r_n} \in \mathcal{X}} \Pr(x_{r_n}|x_s) f(y_{r_n,d}[k_1]|x_{r_n}, y_{r_n,d}[k_2]) \right)$. By approximating the transmission probability term $\Pr(x_{r_n}|x_s)$ using the average SER of the corresponding $S - R_n$ link, denoted as ϵ_n , and applying the widely-used max-sum approximation, the detection rule of NMLD is obtained as

$$\hat{x}_s = \arg \min_{x_s \in \mathcal{X}} \left\{ \frac{1}{N_{s,d}} |y_{s,d}[k_1] - \sqrt{\rho_T/\rho_R} y_{s,d}[k_2] x_s|^2 + \sum_{n=1}^N \min \left\{ \frac{1}{N_{r_n,d}} |y_{r_n,d}[k_1] - \sqrt{\rho_T/\rho_R} y_{r_n,d}[k_2] x_s|^2, \right. \right. \\ \left. \left. \min_{x_{r_n} \in \mathcal{X}} \frac{1}{N_{r_n,d}} |y_{r_n,d}[k_1] - \sqrt{\rho_T/\rho_R} y_{r_n,d}[k_2] x_{r_n}|^2 + \eta_n \right\} \right\}, \quad T \in \{R, N\}, \quad (29)$$

where $\eta_n \triangleq (1 + \rho_T/\rho_R) \log \frac{(1-\epsilon_n)(M-1)}{\epsilon_n}$. Our NMLD is performed based on (29), and the detection procedure is described in **Algorithm 1**. It can be seen from **Algorithm 1** that lines 2-4 have $\mathcal{O}(MN)$ complexity, and so are lines 5-6 (since the cardinality $|\mathcal{X}| = M$) and lines 7-10. Line 11 has $\mathcal{O}(M)$ complexity. Therefore, the overall complexity is $\mathcal{O}(MN)$. The single relay case corresponds to the special case when $N = 1$. Table II shows the number of operations required for the AMLD, the PLD, and the proposed NMLD for detecting one M -DPSK symbol. We can see that the AMLD and PLD have $\mathcal{O}(M^2N)$ and $\mathcal{O}(MN)$ complexities, respectively, while the proposed NMLD has $\mathcal{O}(MN)$ complexity. The total number of operations per symbol detection required for the AMLD and NMLD are $(20M^2 + 2M)N + 19M - 1$ and $(24M - 1)N + 20M - 1$, respectively. An interesting observation is that asymptotically, the overall complexity saving by the NMLD (compared to the AMLD) is up to $\lim_{N \rightarrow \infty} \frac{(20M^2 + 2M)N + 19M - 1 - ((24M - 1)N + 20M - 1)}{(20M^2 + 2M)N + 19M - 1} = 100\% - \frac{24M - 1}{20M^2 + 2M}$, which increases with the modulation size M , and approaches 100% for large enough M .

Algorithm 1: Proposed NMLD for the multiple relay network based on (29)

Input: Received $y_{s,d}[k_1]$, $y_{s,d}[k_2]$, $y_{r_n,d}[k_1]$, and $y_{r_n,d}[k_2]$; Average SERs ϵ_n ;

Power allocation factors ρ_R and ρ_N ; Alphabet \mathcal{X}

Output: Detected source symbol \hat{x}_s

```

1  $\mathcal{X} = \{x_t = e^{j2\pi(t-1)/M}, t = 1, 2, \dots, M\}$ ;
2 for  $n = 1, 2, \dots, N$  do
3   for  $t = 1, 2, \dots, M$  do
4      $\mathbf{F}(n, x_t) \leftarrow \frac{1}{N_{r_n,d}} |y_{r_n,d}[k_1] - \sqrt{\rho_T/\rho_R} y_{r_n,d}[k_2] x_t|^2$ ;
5 for  $n = 1, 2, \dots, N$  do
6    $C_n \leftarrow \min_{x_t \in \mathcal{X}} \mathbf{F}(n, x_t) + \eta_n$ ;
7 for  $t = 1, 2, \dots, M$  do
8   for  $n = 1, 2, \dots, N$  do
9      $\tilde{C}_n(x_t) \leftarrow \min\{\mathbf{F}(n, x_t), C_n\}$ ;
10   $C(x_t) \leftarrow \frac{1}{N_{s,d}} |y_{s,d}[k_1] - \sqrt{\rho_T/\rho_R} y_{s,d}[k_2] x_t|^2 + \sum_{n=1}^N \tilde{C}_n(x_t)$ ;
11  $\hat{x}_s \leftarrow \arg \min_{x_t \in \mathcal{X}} C(x_t)$ ;

```

TABLE II: Number of operations per symbol detection required by AMLD, PLD, and the proposed NMLD for a non-coherent parallel DF relay network with N relays using M -DPSK GDM

Operation Detector	Addition	Multiplication	Max/Min	Exponential/Logarithm
AMLD	$M(9MN - N + 7)$	$M(11MN + 2N + 11)$	$M - 1$	NM
PLD	$(M - 1)(18N + 17)$	$(M - 1)(23N + 23)$	$(M - 1)(2N + 1)$	0
Proposed NMLD	$M(11N + 8)$	$M(11N + 11)$	$(M - 1)(N + 1) + NM$	0

For the rest of the analysis in this section, $L = 1$ is assumed to simplify our presentation even if it is trivial to extend to the case with $L > 1$. It is denoted in (29) that $k_1 = k$, $k_2 = k - 1$, $\sqrt{\rho_T/\rho_R} = 1$ and $\eta_n = 2 \log \frac{(1-\epsilon_n)(M-1)}{\epsilon_n}$.

The NMLD and the PLD are both accurate approximations of the AMLD, and we analyze their relation in Appendix C. Specifically, by proving that the PLD metric can be obtained by approximating the NMLD metric in (29), it is shown that the PLD involves additional approximations compared to the NMLD, for $M > 2$.

B. Pairwise Error Probability

Similarly to the single relay case, the key idea to obtain an SER expression is to determine the dominant PEP terms. The following analysis is provided for calculating the PEP between any two different symbol sets $\mathbf{x}^C = [x_1, x_{r_1}, \dots, x_{r_N}]$ and $\mathbf{x}^E = [x_v, x_{u_1}, \dots, x_{u_N}]$.

Similarly to the single relay case, for all relay-destination links, we define $\omega_{r_n,d}(t_1, t_2) \triangleq \frac{1}{2N_{r_n,d}} (|y_{r_n,d}[k] - y_{r_n,d}[k-1]t_1|^2 - |y_{r_n,d}[k] - y_{r_n,d}[k-1]t_2|^2)$, $n \in \Theta$. Their distributions are obtained as $\omega_{r_n,d}(t_1, t_2) \sim \mathcal{N}(u_{r_n,d}(t_1, t_2), W_{r_n,d}(t_1, t_2))$, where

$$u_{r_n,d}(t_1, t_2) = \gamma_{r_n,d} \operatorname{Re}\{x_{r_n}^*(t_2 - t_1)\}, \quad (30)$$

$$W_{r_n,d}(t_1, t_2) = |t_2 - t_1|^2 \gamma_{r_n,d}. \quad (31)$$

For the n -th branch, the branch metric for a given pair of $(x_s, x_{r_n}), x_{r_n} \neq x_s$, is defined as

$$\min \left\{ \frac{1}{N_{r_n,d}} |y_{r_n,d}[k] - y_{r_n,d}[k-1]x_s|^2, \frac{1}{N_{r_n,d}} |y_{r_n,d}[k] - y_{r_n,d}[k-1]x_{r_n}|^2 + \eta_n \right\}. \quad (32)$$

Solving $\frac{1}{N_{r_n,d}} |y_{r_n,d}[k] - y_{r_n,d}[k-1]x_s|^2 < \frac{1}{N_{r_n,d}} |y_{r_n,d}[k] - y_{r_n,d}[k-1]x_{r_n}|^2 + \eta_n$ gives $\omega_{r_n,d}(x_s, x_{r_n}) < \eta_n/2$. By defining $\tau_n \triangleq \tau_n(x_s, x_{r_n}) = 0$ if $\omega_{r_n,d}(x_s, x_{r_n}) < \eta_n/2$, and 1 otherwise, we can write (32) equivalently as

$$\frac{1}{N_{r_n,d}} |y_{r_n,d}[k] - y_{r_n,d}[k-1](x_s + \tau_n(x_{r_n} - x_s))|^2 + \tau_n \eta_n. \quad (33)$$

Based on (29) and (33), after some manipulations, the detection metric for any given symbol set $\mathbf{x} = [x_s, x_{r_1}, \dots, x_{r_N}]$ can be written as

$$g(\mathbf{x}) = \|\mathbf{V}(\mathbf{y} - \mathbf{Z}(x_s + \mathbf{T}_{\mathbf{x}}(\mathbf{x} - x_s)^T))\|^2 + \|\mathbf{T}_{\mathbf{x}}\tilde{\boldsymbol{\eta}}\|_1, \quad (34)$$

where $\mathbf{V} = \operatorname{diag}\left(\frac{1}{\sqrt{N_{s,d}}}, \frac{1}{\sqrt{N_{r_1,d}}}, \dots, \frac{1}{\sqrt{N_{r_N,d}}}\right)$, $\mathbf{y} = [y_{s,d}[k], y_{r_1,d}[k], \dots, y_{r_N,d}[k]]^T$, $\mathbf{Z} = \operatorname{diag}(y_{s,d}[k-1], y_{r_1,d}[k-1], \dots, y_{r_N,d}[k-1])$, $\tilde{\boldsymbol{\eta}} = [0, \eta_1, \dots, \eta_N]^T$, and $\mathbf{T}_{\mathbf{x}} = \operatorname{diag}(0, \tau_1, \dots, \tau_N)$. Note that in these five matrices and/or vectors, only $\mathbf{T}_{\mathbf{x}}$ is a function of \mathbf{x} .

For $\tilde{\Theta} \subseteq \Theta$, we define $\omega_{\tilde{\Theta}}(\mathbf{x}^C, \mathbf{x}^E) \triangleq \sum_{n \in \tilde{\Theta}} \omega_{r_n,d}((x_1 + \mathbf{T}_{\mathbf{x}^C}(\mathbf{x}^C - x_1)^T)[n], (x_v + \mathbf{T}_{\mathbf{x}^E}(\mathbf{x}^E - x_v)^T)[n]) \sim \mathcal{N}(u_{\tilde{\Theta}}(\mathbf{x}^C, \mathbf{x}^E), W_{\tilde{\Theta}}(\mathbf{x}^C, \mathbf{x}^E))$, with $u_{\tilde{\Theta}}(\mathbf{x}^C, \mathbf{x}^E) \triangleq \sum_{n \in \tilde{\Theta}} u_{r_n,d}((x_1 + \mathbf{T}_{\mathbf{x}^C}(\mathbf{x}^C - x_1)^T)[n], (x_v + \mathbf{T}_{\mathbf{x}^E}(\mathbf{x}^E - x_v)^T)[n])$ and $W_{\tilde{\Theta}}(\mathbf{x}^C, \mathbf{x}^E) \triangleq \sum_{n \in \tilde{\Theta}} W_{r_n,d}((x_1 + \mathbf{T}_{\mathbf{x}^C}(\mathbf{x}^C - x_1)^T)[n], (x_v + \mathbf{T}_{\mathbf{x}^E}(\mathbf{x}^E - x_v)^T)[n])$. Then, based on (34), we have $g(\mathbf{x}^C) - g(\mathbf{x}^E) = \|\mathbf{V}(\mathbf{y} - \mathbf{Z}(x_1 + \mathbf{T}_{\mathbf{x}^C}(\mathbf{x}^C - x_1)^T))\|^2 + \|\mathbf{T}_{\mathbf{x}^C}\tilde{\boldsymbol{\eta}}\|_1 - (\|\mathbf{V}(\mathbf{y} - \mathbf{Z}(x_v + \mathbf{T}_{\mathbf{x}^E}(\mathbf{x}^E - x_v)^T))\|^2 + \|\mathbf{T}_{\mathbf{x}^E}\tilde{\boldsymbol{\eta}}\|_1) = \omega_{s,d}(x_1, x_v) + \omega_{\Theta}(\mathbf{x}^C, \mathbf{x}^E) + \|(\mathbf{T}_{\mathbf{x}^C} - \mathbf{T}_{\mathbf{x}^E})\tilde{\boldsymbol{\eta}}\|_1$. Finally, the PEP for detecting \mathbf{x}^C as \mathbf{x}^E can be obtained as

$$\Pr[g(\mathbf{x}^C) > g(\mathbf{x}^E)] = Q\left(\frac{-u_{s,d}(x_1, x_v) - u_{\Theta}(\mathbf{x}^C, \mathbf{x}^E) - \|(\mathbf{T}_{\mathbf{x}^C} - \mathbf{T}_{\mathbf{x}^E})\tilde{\boldsymbol{\eta}}\|_1}{\sqrt{W_{s,d}(x_1, x_v) + W_{\Theta}(\mathbf{x}^C, \mathbf{x}^E)}}\right).$$

In the following, without loss of generality, we let the relays with index belonging to sets Θ^C and Θ^E detect correctly and wrongly, respectively. The two sets are disjoint and $\Theta^E \cup \Theta^C = \Theta$.

C. SER Performance Analysis

1) *For Error-Free Relaying:* For the scenario of error-free relaying, there is $\Theta^C = \Theta$ and $\Theta^E = \emptyset$, and we have $\mathbf{x}^C = x_1 \mathbf{1}_{N+1}$, and $\mathbf{T}_{\mathbf{x}^C} = \mathbf{0}_{N+1}$. The conditional PEP for detecting \mathbf{x}^C as \mathbf{x}^E is calculated as

$$\begin{aligned} \Pr[g(\mathbf{x}^C) > g(\mathbf{x}^E) | \Theta^C = \Theta, \Theta^E = \emptyset] &= \Pr[\omega_{s,d}(x_1, x_v) + \omega_{\Theta}(\mathbf{x}^C, \mathbf{x}^E) + \|\mathbf{T}_{\mathbf{x}^E} \tilde{\boldsymbol{\eta}}\|_1 > 0] \\ &= Q\left(\frac{-u_{s,d}(x_1, x_v) - u_{\Theta}(\mathbf{x}^C, \mathbf{x}^E) + \|\mathbf{T}_{\mathbf{x}^E} \tilde{\boldsymbol{\eta}}\|_1/2}{\sqrt{W_{s,d}(x_1, x_v) + W_{\Theta}(\mathbf{x}^C, \mathbf{x}^E)}}\right). \end{aligned} \quad (35)$$

Similarly to the single relay case, according to (30) and (31), the problem of maximizing (35) can be written as

$$\begin{aligned} \text{minimize}_{\mathbf{x}^E} \quad & \left(\text{Re}\{1 - x_1^* x_v\} \gamma_{s,d} + \sum_{n=1}^N \text{Re}\{1 - x_1^* (x_v + \tau_n (x_{u_n} - x_v))\} \gamma_{r_n,d} \right)^{\frac{1}{2}} + \\ \text{(P4)} \quad & \frac{\|\mathbf{T}_{\mathbf{x}^E} \tilde{\boldsymbol{\eta}}\|_1}{2} \left(\text{Re}\{1 - x_1^* x_v\} \gamma_{s,d} + \sum_{n=1}^N \text{Re}\{1 - x_1^* (x_v + \tau_n (x_{u_n} - x_v))\} \gamma_{r_n,d} \right)^{-\frac{1}{2}} \\ \text{subject to} \quad & \mathbf{x}^E = [x_v, x_{u_1}, \dots, x_{u_N}] \in \mathcal{X}^{N+1}, x_v \neq x_1. \end{aligned}$$

A dominant case is obtained when $\mathbf{x}^E = x_v \mathbf{1}_N$, and problem (P4) becomes $\text{minimize}_{x_v} \text{Re}\{1 - x_1^* x_v\}$, of which the solution is obtained when $x_v \in \{x_2, x_M\}$. For the analysis of the other values of \mathbf{x}^E , we follow the same logic as the single relay case. Eventually, after some mathematical calculations, the solutions are obtained as: for the n -th branch, if $\tau_n = 0$, then $x_v \in \{x_2, x_M\}$; if $\tau_n = 1$, then $x_v \in \{x_2, x_M\}$ and $x_{u_n} = x_1$. By summing over all dominant PEP terms, an average approximate SER for the scenario of error-free relaying is obtained as

$$\mathcal{P}_e^C \triangleq 2 \prod_{n=1}^N (1 - \epsilon_n) \sum_{m=0}^{N-1} \binom{N}{m} \int Q\left(\sin\left(\frac{\pi}{M}\right) \sqrt{\gamma_m} + \left(\sum_{n=m+1}^N \frac{\eta_n}{4 \sin(\frac{\pi}{M})}\right) \frac{1}{\sqrt{\gamma_m}}\right) p(\gamma_m) d\gamma_m, \quad (36)$$

where m denotes the number of branches with $\tau_n = 0$, and it takes values from 0 to $N - 1$. $\gamma_m \triangleq \gamma_{s,d} + \sum_{n=1}^m \gamma_{r_n,d}$ is gamma distributed. Hereafter, we let $\bar{\gamma}_{s,r_n} = \bar{\gamma}_{r_n,d} = \bar{\gamma}$, $\epsilon_n = \epsilon$, and $\eta_n = \eta$ for $n \in \Theta$. It is derived in Appendix D that

$$\begin{aligned} \mathcal{P}_e^C \approx & 2(1 - \epsilon)^N \sum_{m=0}^{N-1} \binom{N}{m} \frac{1}{2\Gamma(m+1) \bar{\gamma}_m^{m+1}} \frac{2^{-2m-1} ((N-m)\eta)^{m+1} \exp(-(N-m)\eta/4)}{(2 \sin^2(\frac{\pi}{M}) (\sin^2(\frac{\pi}{M})/2 + \bar{\gamma}_m^{-1}))^{\frac{m+1}{2}}} \\ & K_{m+1} \left(\frac{(N-m) \sqrt{\sin^2(\frac{\pi}{M})/2 + \bar{\gamma}_m^{-1}} \eta}{2\sqrt{2} \sin(\frac{\pi}{M})} \right), \end{aligned} \quad (37)$$

where $\bar{\gamma}_m = \frac{m\bar{\gamma} + \bar{\gamma}_{s,d}}{m+1}$ and $K_{m+1}(\cdot)$ is the modified Bessel function of the second kind [32]. Note that this expression applies to the single relay case. We also prove in Appendix D that \mathcal{P}_e^C decays with a rate of $(\ln \bar{\gamma})^{m+\frac{1}{2}}(\bar{\gamma})^{-(N+1)}$, and the full diversity order $N+1$ is achieved for error-free relaying.

2) *For Erroneous Relaying:* Denote $\Theta^E = \{1, 2, \dots, N^E\}$, $N^E \geq 1$, for simplicity, and we have $\mathbf{x}^C = [x_1, x_{r_1}, \dots, x_{r_{N^E}}, x_1 \mathbf{1}_{N^C}]$, $x_{r_n} \neq x_1$ for $n \in \Theta^E$, and $\mathbf{T}_{\mathbf{x}^C} = [0, \mathbf{1}_{N^E}, \mathbf{0}_{N^C}]$. Here, we assume that the detection of the $R_n - D$ link is correct if that of the $S - R_n$ link is wrong [14], and then we have

$$\begin{aligned} \Pr[g(\mathbf{x}^C) > g(\mathbf{x}^E)] &= \Pr[\omega_{s,d}(x_1, x_v) + \omega_{\Theta^C}(\mathbf{x}^C, \mathbf{x}^E) + \omega_{\Theta^E}(\mathbf{x}^C, \mathbf{x}^E) + \|(\mathbf{T}_{\mathbf{x}^C} - \mathbf{T}_{\mathbf{x}^E})\tilde{\boldsymbol{\eta}}\|_1 > 0] \\ &= Q\left(\frac{-u_{s,d}(x_1, x_v) - u_{\Theta^C}(\mathbf{x}^C, \mathbf{x}^E) - u_{\Theta^E}(\mathbf{x}^C, \mathbf{x}^E) - \|(\mathbf{T}_{\mathbf{x}^C} - \mathbf{T}_{\mathbf{x}^E})\tilde{\boldsymbol{\eta}}\|_1/2}{\sqrt{W_{s,d}(x_1, x_v) + W_{\Theta^C}(\mathbf{x}^C, \mathbf{x}^E) + W_{\Theta^E}(\mathbf{x}^C, \mathbf{x}^E)}}\right). \end{aligned} \quad (38)$$

To obtain the dominant PEP terms, we maximize (38) over $\mathbf{T}_{\mathbf{x}^E} \in \{0, 1\}^{N+1}$ with $\mathbf{T}_{\mathbf{x}^E}[1] = 0$. After some involved analysis, the dominant terms are obtained when $\mathbf{T}_{\mathbf{x}^E} = [0, \mathbf{0}_{N^E}, \mathbf{1}_{N^C}]$, $\mathbf{x}^C = [x_1, x_v \mathbf{1}_{N^E}, x_1 \mathbf{1}_{N^C}]$ and $\mathbf{x}^E = [x_v, x_v \mathbf{1}_{N^E}, x_1 \mathbf{1}_{N^C}]$. By adding the multiplicity $\binom{N}{N^E}$, the average approximate SER for this scenario can be obtained as

$$\begin{aligned} \mathcal{P}_e^E &\triangleq \sum_{N^E=1}^N \frac{\binom{N}{N^E}}{M-1} \epsilon^{N^E} (1-\epsilon)^{N-N^E} \sum_{\substack{x_v \in \mathcal{X} \\ x_v \neq x_1}} \int_0^\infty Q\left(\frac{1}{\sqrt{2}} \sqrt{\text{Re}\{1 - x_1^* x_v\} \gamma_{s,d}} + \frac{(N - 2N^E)\eta}{2\sqrt{2} \sqrt{\text{Re}\{1 - x_1^* x_v\} \gamma_{s,d}}}\right) \\ &\quad p(\gamma_{s,d}) d\gamma_{s,d}. \end{aligned} \quad (39)$$

It is derived in Appendix E that

$$\begin{aligned} \mathcal{P}_e^E &\approx \left\{ \sum_{N^E > N/2} \frac{\binom{N}{N^E}}{M-1} \epsilon^{N^E} (1-\epsilon)^{N-N^E} \sum_{\substack{x_v \in \mathcal{X} \\ x_v \neq x_1}} \left[1 - \exp\left(-\frac{(2N^E - N)\eta}{2c_1 \bar{\gamma}_{s,d}}\right) + \frac{(2N^E - N)(4c_1)^{-1/2}\eta}{2(c_1/4 + \bar{\gamma}_{s,d}^{-1})^{1/2} \bar{\gamma}_{s,d}} \right. \right. \\ &\quad \left. \left. K_1\left(\frac{(2N^E - N)\sqrt{c_1/4 + \bar{\gamma}_{s,d}^{-1}}}{2\sqrt{c_1}} \eta\right) \exp((2N^E - N)\eta/4) \right] \right\} + \left\{ \frac{\binom{N}{N/2}}{M-1} \epsilon^{N/2} (1-\epsilon)^{N/2} \sum_{\substack{x_v \in \mathcal{X} \\ x_v \neq x_1}} \frac{2}{4 + c_1 \bar{\gamma}_{s,d}} \right\} \\ &\quad + \left\{ \sum_{N^E < N/2} \frac{\binom{N}{N^E}}{M-1} \epsilon^{N^E} (1-\epsilon)^{N-N^E} \sum_{\substack{x_v \in \mathcal{X} \\ x_v \neq x_1}} \left[\frac{(2N^E - N)(4c_1)^{-1/2}\eta}{2(c_1/4 + \bar{\gamma}_{s,d}^{-1})^{1/2} \bar{\gamma}_{s,d}} K_1\left(\frac{(N - 2N^E)\sqrt{c_1/4 + \bar{\gamma}_{s,d}^{-1}}}{2\sqrt{c_1}} \eta\right) \right. \right. \\ &\quad \left. \left. \exp((2N^E - N)\eta/4) \right] \right\}, \quad 1 \leq N^E \leq N, \end{aligned} \quad (40)$$

where $c_1 = \text{Re}\{1 - x_1^* x_v\} > 0$. Note that this expression applies to the single relay case. We also prove in Appendix E that \mathcal{P}_e^E decays with $(\ln \bar{\gamma})^{\frac{1}{2}}(\bar{\gamma}_{s,d})^{-(N+1-N^E)}$ for $1 \leq N^E \leq \frac{N}{2}$ and with $(\ln \bar{\gamma})^{\frac{1}{2}}(\bar{\gamma}_{s,d})^{-(N^E+1)}$ for $\frac{N}{2} \leq N^E \leq N$, and the diversity order is $\lceil \frac{N}{2} \rceil + 1$. Considering both

scenarios of error-free and erroneous relaying, we give **Proposition 1** to describe the diversity order, where the first part summarizes how the number of erroneous relays affects the diversity order, the second part can be further obtained based on the worst case analysis, and the third part gives the exact diversity order.

Proposition 1. *For the relay network with N parallel DF relays, when M -DPSK is used, the diversity order of both the proposed NMLD and the existing AMLD can be described as follows.*

- *In the case when N^E relays make errors, $0 \leq N^E \leq N$, the diversity order is $d(N^E) = N^E + 1$ if $\frac{N}{2} \leq N^E \leq N$; is $d(N^E) = N + 1 - N^E$ if $0 \leq N^E \leq \frac{N}{2}$.*
- *With r error-free relays, the diversity order is $d = \min_{0 \leq N^E \leq N-r} d(N^E)$.*
- *All cases considered, the achievable diversity order is $d = \left\lceil \frac{N}{2} \right\rceil + 1$.*

Since the NMLD is obtained by applying the accurate max-sum approximation to the AMLD, the average SER and the diversity order expressions derived based on the NMLD are also applicable to the AMLD, which will be verified in Section VI.

Remark 1. *For a multi-branch multi-hop non-coherent DF relay network, assume there are N parallel branches, and each branch has U hops. Denote the u -th relay of the n -th branch as $R_{n,u}$, $n \in \{1, 2, \dots, N\}$, $u \in \{1, 2, \dots, U-1\}$. Then, according to [33], the multi-hop branch $S - R_{n,1} - R_{n,2} - \dots - R_{n,U-1}$ can be transformed into an equivalent single-hop link $S - R_{n,U-1}$ in terms of the average SER and the diversity order. Thanks to this, the proposed NMLD detection metric in (29) can be applied to this network by replacing $y_{r_n,d}$ with $y_{r_{n,U-1},d}$, $n \in \{1, 2, \dots, N\}$, where $y_{r_{n,U-1},d}$ denotes the received signal at the destination from $R_{n,U-1}$. In this case, ϵ_n is the average SER at $R_{n,U-1}$ (for the equivalent single-hop link $S - R_{n,U-1}$). It can be calculated according to [33]. Besides, the proposed performance analysis method remains valid due to the aforementioned multi-hop to single-hop equivalence transformation.*

VI. SIMULATION RESULTS

This section presents simulation results in the cases of single- and multi-relay networks. For comparison, the results in the coherent counterparts are also presented using the coherent AMLD in [15]. For this coherent counterpart, the CSI assumption is: each relay has the perfect instantaneous CSI of the corresponding source-relay link, and the destination has the perfect

instantaneous CSI of the source/relay-destination links, but only the average CSI of the source-relay links. Let all nodes transmit with the same power $P_s = 1$. As mentioned in Section II-A, we consider quasi-static Rayleigh fading, that is, each channel coefficient $h_{I,J}$, $(I, J) \in \{(s, r), (s, d), (r, d)\}$, remains unchanged within one frame (K symbols) duration, while varies independently from one frame to another. The default simulation settings are as follows unless specified otherwise. The modulation used is QPSK, $(\rho_R, \rho_N) = (\rho_R^*, \rho_N^*)$ as in (28), all links have the same average SNR $\bar{\gamma}$, i.e., $\bar{\gamma}_{s,d} = \bar{\gamma}_{s,r_n} = \bar{\gamma}_{r_n,d} = \bar{\gamma}$, and we set $N_{s,d} = N_{s,r_n} = N_{r_n,d} = N_0 = 1$, $n \in \Theta$.

A. Single Relay Network

Fig. 3 compares the SER performance of various schemes when the information frame length $K = 320$ and block length $L = 16$. It is seen that the proposed NMLD-GDM outperforms the AMLD-DM and PLD-DM. For example, to achieve an SER of 10^{-3} using 8-PSK, the performance gap between NMLD-GDM and AMLD(PLD)-DM is around 2 dB. In addition, the proposed SER expression is shown to be accurate for all three values of M over the whole SNR range. Fig. 4 shows the complexity comparison of various schemes with different modulation size $M \in \{2, 4, 8, 16\}$. Fig. 4(a) compares the average run time in Matlab, while Fig. 4(b) compares the total number of operations (c.f. Table II). For the run time comparison, the average SNR $\bar{\gamma} = 20$ dB, and 10^4 symbol detections are performed for each value of M using each detector under consideration. We can see that the run time (and the total number of operations) of the proposed NMLD is linear in M , while those of the AMLD and PLD are quadratic and linear in M , respectively. This agrees with the complexity order analysis in Table II. Together with the SER comparison in Fig. 3, it can be seen that the proposed NMLD-GDM outperforms the AMLD-DM with a reduced complexity order.

Fig. 5(a) shows the impact of the block length L on the SER performance when $K = 512$. The SER of the coherent counterpart is presented as a lower bound, while that of the DM scheme (the $L = 1$ case) as an upper bound. It is observed that by increasing the block length L , the SER performance can be significantly improved, and can be close to that of the coherent counterpart. For example, when $L = 256$, the performance gap with the coherent scheme is within 0.5 dB. Fig. 5(b) shows the SER performance with respect to $\rho_N \in (0, 1)$ when $\bar{\gamma} = 10$ and 20 dB. According to (28), when $L = 8$ and 256, we have $\rho_N^* = 0.830$ and 0.945, respectively. The simulate SERs for using these two optimized values are also shown in solid stars. It is obvious that for

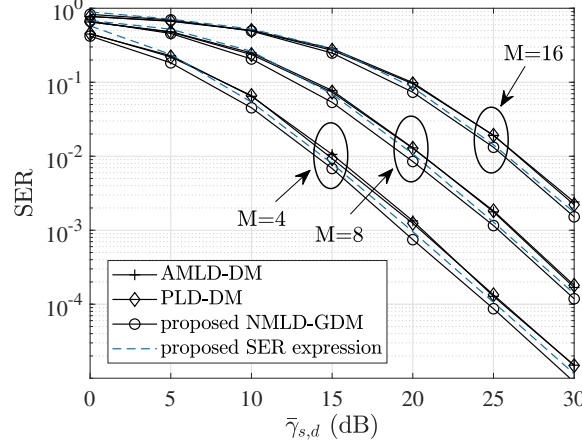


Fig. 3: SER performance comparison of various schemes and the proposed SER expression using M -DPSK when the information frame length $K = 320$ and the block length $L = 16$ in the non-coherent DF single relay network under quasi-static Rayleigh fading (the fading coefficients remain fixed for the duration of one frame, while vary independently from one frame to another).

both cases when $\bar{\gamma} = 10$ and 20 dB, the simulate SERs of GDM with $L = 8$ and 256 show unique minimums, which are around the optimized values ρ_N^* calculated using (28). This verifies that the solution in (28) is accurate from middle to high SNR values. Let us take a closer look at the case of $\bar{\gamma} = 20$ dB. It can be seen that the SERs of DM and the coherent counterpart do not change with ρ_N , since no power allocation is exploited. With improper power allocation, such as when $\rho_N < 0.5$, the SER performance for GDM is shown to be worse than that of DM. By contrast, with proper power allocation, such as when $\rho_N > 0.6$, GDM is shown to outperform DM. In the case when $L = 256$, the proposed scheme with $\rho_N^* = 0.945$ (see the solid red star) performs close to the coherent counterpart, which agrees with the earlier observations in Fig. 5(a). It is also seen that with $\rho_N = 1$ (the RSs and NSs are allocated the same power P_s), the SER of GDM is the same as that of DM, saying that the conventional DM is a special case of the GDM scheme.

B. Multiple Relay Networks

In the multi-relay networks, to focus on the SER performance of the proposed NMLD, we adopt the conventional DM scheme without exploiting power allocation.

Fig. 6 shows the performance and complexity comparisons with different relay number N using 8-DPSK. Fig. 6(a) shows the simulate SERs of the AMLD, the PLD and the proposed

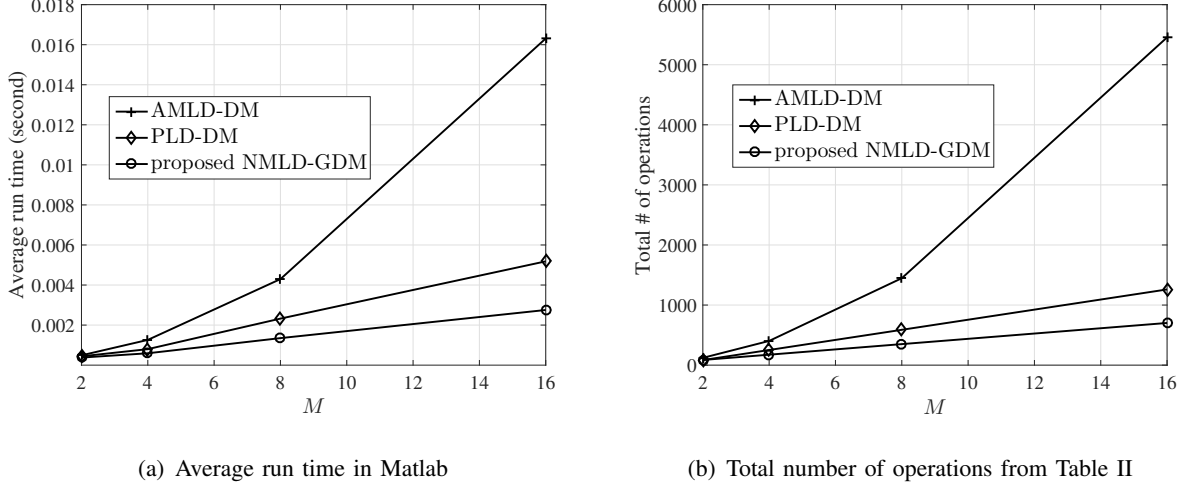


Fig. 4: Detection complexity comparison of various schemes using M -DPSK in the non-coherent DF single relay network under quasi-static Rayleigh fading (the fading coefficients remain fixed for the duration of one frame, while vary independently from one frame to another).

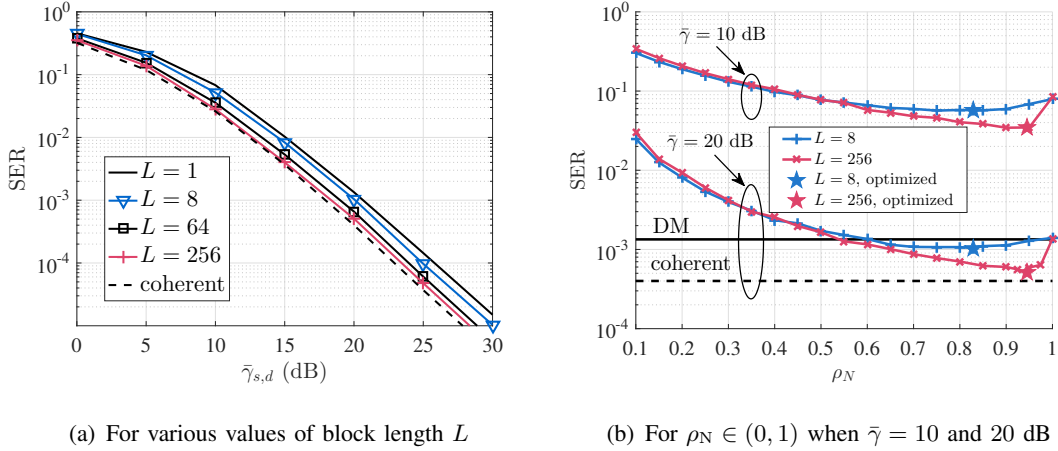


Fig. 5: SER performance comparison using the proposed NMLD when the information frame length $K = 512$ in the non-coherent DF single relay network using QPSK under quasi-static Rayleigh fading. The SER of the coherent counterpart is presented as a lower bound.

NMLD with $N \in \{2, 3, 4, 6\}$ DF relays, when $\bar{\gamma}_{s,r_n} = \bar{\gamma}_{r_n,d} = \bar{\gamma}_{s,d} + 10$ dB, $n = 1, 2, \dots, N$, for 8-DPSK signals. The proposed SER expression in (37) and (40) is also plotted to show its accuracy. We can see that the SER performance of the NMLD is nearly the same as that of the AMLD. Besides, the SER expression is verified to be very accurate for all values of N . Meanwhile,

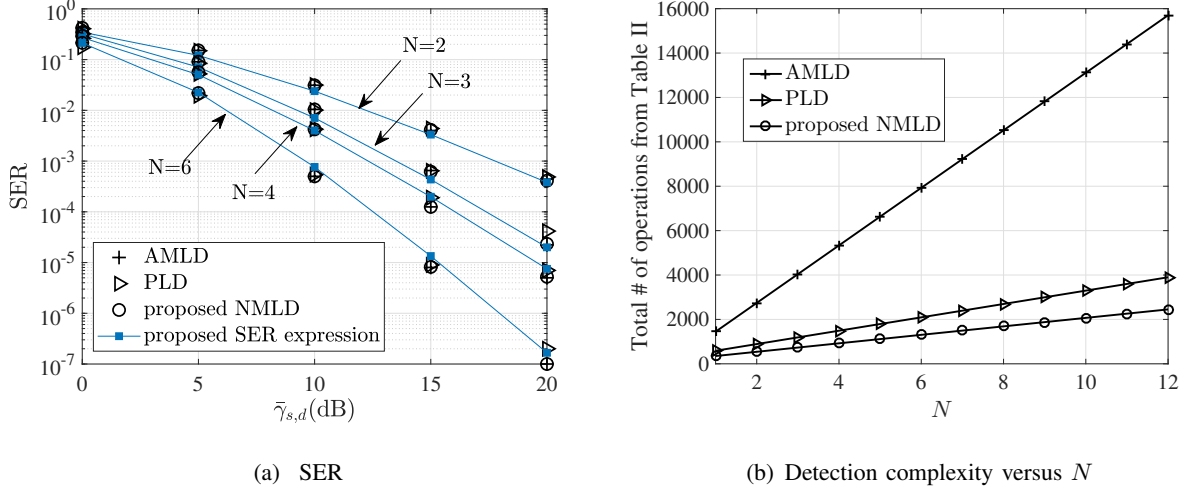
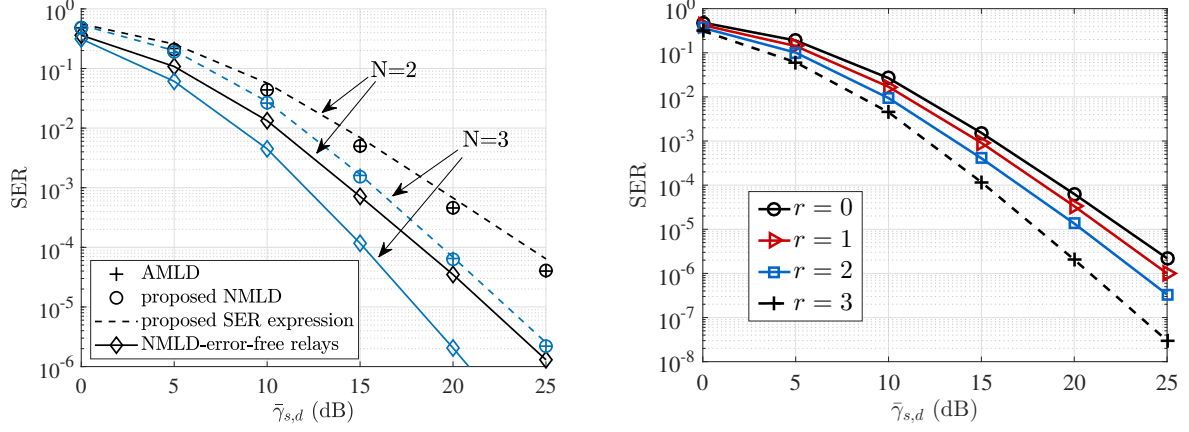


Fig. 6: SER performance and detection complexity comparisons of various detectors in the non-coherent DF parallel relay network with N relays using 8-DPSK DM for $\bar{\gamma}_{s,r_n} = \bar{\gamma}_{r_n,d} = \bar{\gamma}_{s,d} + 10$ dB and $n = 1, 2, \dots, N$.

we can see that for both the AMLD and NMLD, the achievable diversity order for $N = 2$ is 2, for $N = 3$ is 3, for $N = 4$ is 3, and for $N = 6$ is 4, which are in exact agreement with the proposed diversity order expression $\left\lceil \frac{N}{2} \right\rceil + 1$. An interesting observation is that for infinite N , we have $\lim_{N \rightarrow \infty} \frac{\text{achievable diversity order}}{\text{full diversity order}} = \lim_{N \rightarrow \infty} \frac{\left\lceil \frac{N}{2} \right\rceil + 1}{N+1} = \frac{1}{2}$, which means that asymptotically only half of the full diversity is achievable. Fig. 6(b) compares the total number of operations (c.f. Table II) with respect to N . It can be seen that all three detectors have linear complexities in N , but the proposed NMLD can save a considerable number of operations. For example, when $N = 12$, the complexity saving by the NMLD (compared to the AMLD) is up to $\frac{15703-2451}{15703} = 84.39\%$. Overall, the proposed NMLD can achieve similar performance as the AMLD but with a considerably reduced complexity.

Fig. 7(a) shows the SER performances of the AMLD and the proposed NMLD in the non-coherent DF relay networks with $N = 2$ and 3 parallel relays. It is seen that the NMLD achieves almost the same SER performance as the AMLD, and the proposed SER expression calculated from (37) and (40) is accurate. Moreover, it is shown that both the NMLD and the AMLD achieve exactly the proposed diversity order $\left\lceil \frac{N}{2} \right\rceil + 1$, while when all relays are error-free, the NMLD achieves the full diversity order $N + 1$. Fig. 7(b) further shows the simulate SERs of the AMLD with r error-free relays when $N = 3$. It is seen that for $r = 0, 1$ and 2, the AMLD



(a) For comparison of the AMLD and the proposed NMLD when $N = 2$ and 3 (b) For the AMLD with r error-free relays when $N = 3$

Fig. 7: SER performance of various detectors for the conventional DM in the non-coherent DF multiple relay networks with N parallel relays using DQPSK.

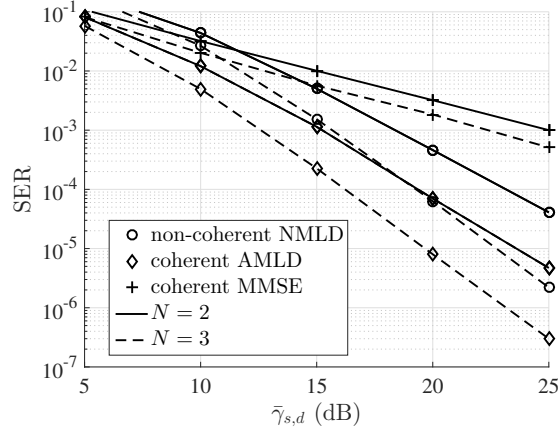


Fig. 8: SER performance comparison of various detectors in the non-coherent (using the conventional DM) and coherent DF relay networks with $N \in \{2, 3\}$ parallel relays using QPSK.

achieves the diversity order 3, while for $r = 3$, the full diversity order 4 can be achieved. The results are in exact agreement with the second part of **Proposition 1**.

Fig. 8 compares the simulate SERs in non-coherent and coherent relay networks for $N = 2$ and 3. The AMLD in [15] (called the coherent AMLD) and the minimum mean squared error (MMSE) detector are used for the coherent case, for which the CSI assumption is described at the beginning of this section. The MMSE detector is one of the most practical linear-complexity

detector. We can see that the non-coherent NMLD largely outperforms the coherent MMSE detector at SERs below 10^{-2} . The MMSE detector ignores the relay detection errors, which results in its poor performance. For each value of N , it can be observed that the SERs of the non-coherent NMLD and coherent AMLD decay at nearly the same rate, but the former suffers about 3 dB performance loss as compared to the later. It was proved in [14] that if we assume the instantaneous CSI of all links to be available at the destination, coherent detection can achieve the full diversity order $N + 1$. Unlike this, the coherent AMLD considered here assumes the availability of the average (instead of the instantaneous) CSI of the source-relay links at the destination. It is seen from Fig. 8 that the coherent AMLD achieves the diversity order $\left\lceil \frac{N}{2} \right\rceil + 1$. Moreover, the non-coherent NMLD is shown to achieve the same diversity order $\left\lceil \frac{N}{2} \right\rceil + 1$ as the coherent AMLD.

VII. CONCLUSION

In this work, we proposed a new detector, i.e., the NMLD, for the non-coherent relay network with N parallel DF relays using GDM based on M -PSK. An accurate SER expression was then derived, and based on which an optimized transmission power allocation scheme was designed. Simulation results showed that the proposed non-coherent scheme can greatly reduce the performance gap between the conventional non-coherent DM scheme and the coherent counterpart. For example, for a block length of 256 symbols at SER 10^{-5} using DQPSK in the single relay case, the gap was reduced from approximately 3 dB to within 0.5 dB. Moreover, by analyzing the behavior of the SER expression at high SNR, it was proved that the diversity order of both the proposed NMLD and the state-of-the-art AMLD is exactly $\left\lceil \frac{N}{2} \right\rceil + 1$. The accuracy of the diversity order was further confirmed by extensive simulation, revealing that the full diversity order $N + 1$ is not achievable for $N > 1$.

APPENDIX

A. Expression of ϵ

An expression of the average SER for M -PSK using coherent detection over a Rayleigh fading channel is obtained in [34, eq. (8.112)] as $\mathcal{P}_e^{\text{co}}(\bar{\gamma}) = \frac{M-1}{M} - \sqrt{\frac{\bar{\gamma} \sin^2(\frac{\pi}{M})}{1 + \bar{\gamma} \sin^2(\frac{\pi}{M})}} \times \left[\frac{1}{2} + \frac{1}{\pi} \tan^{-1} \left(\sqrt{\frac{\bar{\gamma} \sin^2(\frac{\pi}{M})}{1 + \bar{\gamma} \sin^2(\frac{\pi}{M})}} \cot \frac{\pi}{M} \right) \right]$, with $\bar{\gamma}$ denoting the average SNR. By using the average receive SNR $\phi_T \bar{\gamma}_{s,r} = \frac{1}{1/\rho_T + 1/\rho_R} \bar{\gamma}_{s,r}$, $T \in \{R, N\}$, obtained in (10) to replace $\bar{\gamma}$ in this expression, we obtain

$$\epsilon = (1/L) \mathcal{P}_e^{\text{co}}(\phi_R \bar{\gamma}_{s,r}) + (1 - 1/L) \mathcal{P}_e^{\text{co}}(\phi_N \bar{\gamma}_{s,r}). \quad (41)$$

B. Monotonicity of the Second Term in (25)

Denote $z = \sin(\frac{\pi}{M})\sqrt{2\phi_N} > 0$ and $q(z) = z\sqrt{\gamma_{s,d}} - \frac{\log \frac{(1-\epsilon)(M-1)}{\epsilon}}{2z\sqrt{\gamma_{s,d}}}$. The second term in (25) can be written as $\tilde{\mathcal{P}}_N^E(z) = \frac{2\epsilon}{M-1}Q(q(z))$ for NSs.³ For $\tilde{\mathcal{P}}_N^E(z)$ to be decreasing in z (equivalently, in ϕ_N), by taking derivative, a sufficient and necessary condition is obtained as $\frac{\partial \tilde{\mathcal{P}}_N^E(z)}{\partial z} = \frac{\partial \epsilon}{\partial z}Q(q(z)) + \epsilon \partial Q(q(z))/\partial z < 0$. Since $\frac{\log \frac{(1-\epsilon)(M-1)}{\epsilon}}{2z^2\gamma_{s,d}} \rightarrow \infty \implies \frac{\log \frac{(1-\epsilon)(M-1)}{\epsilon}}{2z^2\gamma_{s,d}} \gg 1 \iff \frac{\log \frac{(1-\epsilon)(M-1)}{\epsilon}}{2z\sqrt{\gamma_{s,d}}} \gg z\sqrt{\gamma_{s,d}}$, we have $q(z) \approx -\frac{\log \frac{(1-\epsilon)(M-1)}{\epsilon}}{2z\sqrt{\gamma_{s,d}}} < 0$. By applying this to the derivative $\frac{\partial \tilde{\mathcal{P}}_N^E(z)}{\partial z}$ and then using $Q(x) \approx \frac{1}{2}e^{-\frac{x^2}{2}}$, $x > 0$, the sufficient and necessary condition can be written as

$$-\frac{\epsilon \log^2 \frac{(1-\epsilon)(M-1)}{\epsilon}}{4z^3\gamma_{s,d}} + [2 \exp(\frac{\log^2 \frac{(1-\epsilon)(M-1)}{\epsilon}}{8z^2\gamma_{s,d}}) - \frac{\log \frac{(1-\epsilon)(M-1)}{\epsilon}}{4z^2\gamma_{s,d}} - 1] \frac{\partial \epsilon}{\partial z} < 0. \quad (42)$$

Note that $\frac{\partial \epsilon}{\partial z} < 0$. By ignoring the first summation term (which is negative) in the left hand side (LHS) of (42) and rearranging the terms, a sufficient condition is obtained as $\sqrt{M-1}^{-\frac{z_0}{2}} \left(1 + \frac{z_0}{2}\right) < 2\epsilon^{-\frac{z_0}{4}}$, where $z_0 = \frac{\log \frac{(1-\epsilon)(M-1)}{\epsilon}}{2z^2\gamma_{s,d}}$ (for notational convenience). Next, we prove that this sufficient condition holds true when $z_0 \rightarrow \infty$. For the LHS, we have $\lim_{z_0 \rightarrow \infty} \sqrt{M-1}^{-\frac{z_0}{2}} \left(1 + \frac{z_0}{2}\right) = 0$. For the right hand side, since $0 < \epsilon < 1$ and $z_0 > 0$, we have $2\epsilon^{-\frac{z_0}{4}} > 2$. Therefore, the sufficient condition holds true when $z_0 \rightarrow \infty$. Overall, provided that $\frac{\log \frac{(1-\epsilon)(M-1)}{\epsilon}}{2z^2\gamma_{s,d}} \rightarrow \infty$ holds true, $\tilde{\mathcal{P}}_N^E(z)$ is monotonically decreasing in z , and equivalently, in ϕ_N .

C. Relationship between the NMLD and the PLD

Note that for a clear comparison, we follow the notations and definitions in [30] as closely as possible. Let x_p and x_q denote a given pair of any two different symbols belonging to \mathcal{X} . By reducing the candidate set of the relay symbols from \mathcal{X}^N to $\{x_p, x_q\}^N$ for $M > 2$, the NMLD detection metric in (29) can be approximated using $\beta^{I,J}$, $I \in \{p, q\}$, $J = \{p, q\} \setminus I$, as $\beta^{I,J} = \frac{1}{N_{s,d}}|y_{s,d}[k] - y_{s,d}[k-1]x_I|^2 + \sum_{n=1}^N \min \left\{ \frac{1}{N_{r_n,d}}|y_{r_n,d}[k] - y_{r_n,d}[k-1]x_I|^2, \min_{x_{r_n} \in \{x_p, x_q\}} \frac{1}{N_{r_n,d}}|y_{r_n,d}[k] - y_{r_n,d}[k-1]x_{r_n}|^2 + \eta_n \right\}$. After some algebra, we have

$$\beta^{p,q} = \frac{1}{N_{s,d}}|y_{s,d}[k] - y_{s,d}[k-1]x_p|^2 + \sum_{n=1}^N \begin{cases} \frac{1}{N_{r_n,d}}|y_{r_n,d}[k] - y_{r_n,d}[k-1]x_p|^2, & \text{if } t_n \geq -\frac{\eta_n}{2}, \\ \frac{1}{N_{r_n,d}}|y_{r_n,d}[k] - y_{r_n,d}[k-1]x_q|^2 + \eta_n, & \text{if } t_n < -\frac{\eta_n}{2}, \end{cases} \quad (43)$$

and

$$\beta^{q,p} = \frac{1}{N_{s,d}}|y_{s,d}[k] - y_{s,d}[k-1]x_q|^2 + \sum_{n=1}^N \begin{cases} \frac{1}{N_{r_n,d}}|y_{r_n,d}[k] - y_{r_n,d}[k-1]x_q|^2, & \text{if } t_n \leq \frac{\eta_n}{2}, \\ \frac{1}{N_{r_n,d}}|y_{r_n,d}[k] - y_{r_n,d}[k-1]x_p|^2 + \eta_n, & \text{if } t_n > \frac{\eta_n}{2}, \end{cases} \quad (44)$$

³For presentational convenience, $M > 2$ is considered, but the analysis of $M = 2$ is only slightly different.

where $t_n = \frac{1}{N_{r_n,d}} \text{Re}\{y_{r_n,d}^*[k]y_{r_n,d}[k-1](x_p - x_q)\}$. Then, based on (43) and (44), the detection metric of the PLD is obtained as

$$\Lambda^{p,q} \triangleq \beta^{q,p} - \beta^{p,q} = t_0 + \sum_{n=1}^N \begin{cases} -\frac{\eta_n}{2}, & \text{if } t_n < -\frac{\eta_n}{2}, \\ t_n & \text{if } -\frac{\eta_n}{2} \leq t_n \leq \frac{\eta_n}{2}, \\ \frac{\eta_n}{2}, & \text{if } t_n > \frac{\eta_n}{2}, \end{cases}$$

where $t_0 = \frac{1}{N_{s,d}} \text{Re}\{y_{s,d}^*[k]y_{s,d}[k-1](x_p - x_q)\}$ and $\Lambda^{p,q}$ is the log-likelihood ratio between x_p and x_q . Note that when $M = 2$, the detection metrics of the PLD and the NMLD are exact the same.

D. Approximate Average SER and Diversity Order Analysis for Error-Free Relaying

\mathcal{P}_e^C in (36) can be written as $2(1 - \epsilon)^N \sum_{m=0}^{N-1} \binom{N}{m} \int_0^\infty Q\left(\sin\left(\frac{\pi}{M}\right)\sqrt{\gamma_m} + \frac{(N-m)\eta}{4\sin\left(\frac{\pi}{M}\right)}\frac{1}{\sqrt{\gamma_m}}\right)p(\gamma_m) d\gamma_m$, with $p(\gamma_m) = \frac{(\gamma_m)^m}{\Gamma(m+1)\bar{\gamma}_m^{m+1}}e^{-\frac{\gamma_m}{\bar{\gamma}_m}}$. By applying $Q(x) \approx \frac{1}{2}e^{-\frac{x^2}{2}}$ to the integral term in \mathcal{P}_e^C , we have

$$\begin{aligned} & \int_0^\infty Q\left(\sin\left(\frac{\pi}{M}\right)\sqrt{\gamma_m} + \frac{(N-m)\eta}{4\sin\left(\frac{\pi}{M}\right)}\frac{1}{\sqrt{\gamma_m}}\right)p(\gamma_m) d\gamma_m \\ & \approx \frac{1}{2\Gamma(m+1)\bar{\gamma}_m^{m+1}} \int_0^\infty \exp\left(-\frac{(2\sin^2\left(\frac{\pi}{M}\right)\gamma_m + (N-m)\eta/2)^2}{8\sin^2\left(\frac{\pi}{M}\right)\gamma_m}\right)(\gamma_m)^m e^{-\frac{\gamma_m}{\bar{\gamma}_m}} d\gamma_m. \end{aligned} \quad (45)$$

For the integral term in (45) we have

$$\begin{aligned} & \int_0^\infty \exp\left(-\frac{(2\sin^2\left(\frac{\pi}{M}\right)\gamma_m + (N-m)\eta/2)^2}{8\sin^2\left(\frac{\pi}{M}\right)\gamma_m}\right)(\gamma_m)^m e^{-\frac{\gamma_m}{\bar{\gamma}_m}} d\gamma_m \\ & = \frac{2^{-2m-1}((N-m)\eta)^{m+1} \exp(-(N-m)\eta/4)}{(2\sin^2\left(\frac{\pi}{M}\right)(\sin^2\left(\frac{\pi}{M}\right)/2 + \bar{\gamma}_m^{-1}))^{\frac{m+1}{2}}} K_{m+1}\left(\frac{(N-m)\sqrt{\sin^2\left(\frac{\pi}{M}\right)/2 + \bar{\gamma}_m^{-1}}\eta}{2\sqrt{2}\sin\left(\frac{\pi}{M}\right)}\right) \end{aligned} \quad (46)$$

$$\begin{aligned} & \approx \sqrt{\pi} 2^{-2m} \sin^{-m-\frac{1}{2}}\left(\frac{\pi}{M}\right) ((N-m)\eta)^{m+\frac{1}{2}} (\sin^2\left(\frac{\pi}{M}\right)/2 + \bar{\gamma}_m^{-1})^{-\frac{m}{2}-\frac{3}{4}} \exp(-(N-m)\eta/4) \\ & \quad \exp\left(-(N-m)\sqrt{\sin^2(\pi/M)/2 + \bar{\gamma}_m^{-1}}\eta/(2\sqrt{2}\sin(\pi/M))\right) \end{aligned} \quad (47)$$

$$\propto (\ln \bar{\gamma}_m)^{m+\frac{1}{2}} (\bar{\gamma}_m)^{-(N-m)}. \quad (48)$$

(46) is obtained based on [35], and we obtain (37). Next, we show how to obtain (47). By applying the binomial theorem, we have $\lim_{\bar{\gamma}_m \rightarrow \infty} (\sin^2\left(\frac{\pi}{M}\right)/2 + \bar{\gamma}_m^{-1})^{1/2} = (\sin^2\left(\frac{\pi}{M}\right)/2)^{1/2} + \frac{1}{2}(\sin^2\left(\frac{\pi}{M}\right)/2)^{-1/2}\bar{\gamma}_m^{-1}$.

Then for the term inside the Bessel function $K_{m+1}(\cdot)$, we have $\lim_{\bar{\gamma}_m \rightarrow \infty} (N-m)\eta(\sin^2\left(\frac{\pi}{M}\right)/2 + \bar{\gamma}_m^{-1})^{1/2} \sin^{-1}\left(\frac{\pi}{M}\right) = \lim_{\bar{\gamma}_m \rightarrow \infty} c_0((\sin^2\left(\frac{\pi}{M}\right)/2)^{1/2} + \frac{1}{2}(\sin^2\left(\frac{\pi}{M}\right)/2)^{-1/2}\bar{\gamma}_m^{-1}) \ln \bar{\gamma}_m = c_0(\sin^2\left(\frac{\pi}{M}\right)/2)^{1/2} \ln \bar{\gamma}_m \gg 0$ with c_0 denoting some positive constant. Therefore based on $K_1(x) \approx (\pi/2)^{1/2}x^{-1/2}\exp(-x)$ when $x \gg 0$, we can approximate the $K_{m+1}(\cdot)$ term and obtain (47). Finally, accordingly to \mathcal{P}_e^C and (48), it is concluded that for error-free relaying, \mathcal{P}_e^C decays with $(\ln \bar{\gamma}_m)^{m+\frac{1}{2}}(\bar{\gamma}_m)^{-(N-m)}(\bar{\gamma}_m)^{-(m+1)} = (\ln \bar{\gamma}_m)^{m+\frac{1}{2}}(\bar{\gamma}_m)^{-(N+1)}$, and the proposed NMLD achieves the full diversity order $N + 1$.

E. Approximate Average SER and Diversity Order Analysis for Erroneous Relaying

First, we analyze the case when $2N^E - N > 0$, i.e., the number of erroneous relays is larger than that of error-free ones. By applying $Q(x) \approx \frac{1}{2}e^{-\frac{x^2}{2}}$, we have

$$\begin{aligned} & \frac{1}{\bar{\gamma}_{s,d}} \int_0^\infty Q\left(\sqrt{\frac{c_1}{2}}\sqrt{\gamma_{s,d}} - \frac{(2N^E - N)\eta}{2\sqrt{2c_1}}\frac{1}{\sqrt{\gamma_{s,d}}}\right) \exp\left(-\frac{\gamma_{s,d}}{\bar{\gamma}_{s,d}}\right) d\gamma_{s,d} \\ & \approx \frac{1}{\bar{\gamma}_{s,d}} \int_0^{\frac{(2N^E - N)\eta}{2c_1}} \exp\left(-\frac{\gamma_{s,d}}{\bar{\gamma}_{s,d}}\right) d\gamma_{s,d} + \frac{1}{2\bar{\gamma}_{s,d}} \int_{\frac{(2N^E - N)\eta}{2c_1}}^\infty \exp\left(-\frac{(c_1\gamma_{s,d} - \frac{2N^E - N}{2}\eta)^2}{4c_1\gamma_{s,d}}\right) \exp\left(-\frac{\gamma_{s,d}}{\bar{\gamma}_{s,d}}\right) d\gamma_{s,d} \end{aligned}$$

where $c_1 = \text{Re}\{1 - x_1^* x_v\} > 0$. Z_1 and Z_2 are used to represent the first and second summation terms, respectively. We have $Z_1 = 1 - \exp\left(-\frac{(2N^E - N)\eta}{2c_1\bar{\gamma}_{s,d}}\right)$, and $\lim_{\bar{\gamma}_{s,d}=\bar{\gamma} \rightarrow \infty} Z_1 = 1 - \lim_{\bar{\gamma} \rightarrow \infty} \exp\left(-\frac{(2N^E - N)\eta}{2c_1\bar{\gamma}}\right) = 1 - \exp\left(-c_2 \lim_{\bar{\gamma} \rightarrow \infty} \frac{\ln \bar{\gamma}}{\bar{\gamma}}\right) = 0$ with c_2 denoting some positive constant. Now we deal with Z_2 , which can be written as

$$Z_2 \approx \frac{1}{2\bar{\gamma}_{s,d}} \int_0^\infty \exp\left(-\frac{(c_1\gamma_{s,d} - \frac{2N^E - N}{2}\eta)^2}{4c_1\gamma_{s,d}}\right) \exp\left(-\frac{\gamma_{s,d}}{\bar{\gamma}_{s,d}}\right) d\gamma_{s,d} \quad (49)$$

$$\begin{aligned} & = \frac{(2N^E - N)(4c_1)^{-1/2}\eta}{2\left(c_1/4 + \bar{\gamma}_{s,d}^{-1}\right)^{1/2}\bar{\gamma}_{s,d}} K_1\left(\frac{(2N^E - N)\sqrt{c_1/4 + \bar{\gamma}_{s,d}^{-1}}}{2\sqrt{c_1}}\eta\right) \exp\left((2N^E - N)\eta/4\right) \\ & = V_1 V_2 V_3, \end{aligned} \quad (50)$$

where $V_1 \triangleq \frac{(2N^E - N)(4c_1)^{-1/2}\eta}{2\left(c_1/4 + \bar{\gamma}_{s,d}^{-1}\right)^{1/2}\bar{\gamma}_{s,d}}$, $V_2 \triangleq K_1(\cdot)$ and $V_3 \triangleq \exp((2N^E - N)\eta/4)$. (49) is obtained by approximating Z_2 using an upper bound. It can be numerically shown that the value of (49) is very close to Z_2 , and therefore it is an accurate approximation. Similarly to (46), (50) is obtained based on [35], and we obtain the expression in the first curly bracket of (40). Now we analyze the diversity order. As $\bar{\gamma}_{s,d} \rightarrow \infty$, based on $K_1(z) \approx (\pi/2)^{1/2} z^{-1/2} \exp(-z)$ when $z \gg 0$, we can get

$$\begin{aligned} V_2 & \approx (\pi/4)^{1/2} \left((2N^E - N)\eta/2\right)^{-1/2} (4c_1)^{1/4} \left(c_1/4 + \bar{\gamma}_{s,d}^{-1}\right)^{-1/4} \exp\left(-\frac{(2N^E - N)\sqrt{c_1/4 + \bar{\gamma}_{s,d}^{-1}}}{2\sqrt{c_1}}\eta\right), \\ V_1 V_2 & \propto (\ln \bar{\gamma})^{\frac{1}{2}} \left(c_1/4 + \bar{\gamma}_{s,d}^{-1}\right)^{-3/4} \bar{\gamma}_{s,d}^{-1} (\bar{\gamma}_{s,d})^{-2(2N^E - N)(4c_1)^{-1/2}(c_1/4 + \bar{\gamma}_{s,d}^{-1})^{1/2}} \\ & \propto (\ln \bar{\gamma})^{\frac{1}{2}} \bar{\gamma}_{s,d}^{-1} (\bar{\gamma}_{s,d})^{-\frac{2N^E - N}{2}}. \end{aligned}$$

It is straightforward to show that $V_3 \propto (\bar{\gamma}_{s,d})^{\frac{2N^E - N}{2}}$, and then we have $V_1 V_2 V_3 \propto (\ln \bar{\gamma})^{\frac{1}{2}} \bar{\gamma}_{s,d}^{-1}$. Therefore \mathcal{P}_e^E decays with $(\ln \bar{\gamma})^{\frac{1}{2}} (\bar{\gamma}_{s,d})^{-(N^E + 1)}$. Considering the constraint that $2N^E - N > 0$, the diversity order is determined by the worst case when $N^E = \left\lfloor \frac{N}{2} \right\rfloor + 1$. So it is $\frac{N}{2} + 2$ and $\frac{N+1}{2} + 1$, respectively, for even and odd N .

When $2N^E - N = 0$, similarly we can obtain $Z_1 = 0$ and $Z_2 = \frac{2}{4 + c_1\bar{\gamma}_{s,d}}$. Then the expression in the second curly bracket of (40) can be obtained. When $2N^E - N < 0$, similarly to the error-free

relaying case, the expression in the third curly bracket of (40) can be obtained. After some calculation, it can be shown that \mathcal{P}_e^E decays with $(\ln \bar{\gamma})^{\frac{1}{2}} (\bar{\gamma}_{s,d})^{-(N+1-N^E)}$ for $2N^E - N \leq 0$, and therefore the diversity order is $N + 1 - N^E$. Considering $2N^E - N \leq 0$, the diversity order is determined by the worst case when $N^E = \left\lfloor \frac{N}{2} \right\rfloor$. So it is $\frac{N}{2} + 1$ and $\frac{N+1}{2} + 1$, respectively, for even and odd N . Overall speaking, for erroneous relaying, we obtain the diversity as $\frac{N}{2} + 1$ and $\frac{N+1}{2} + 1$, for even and odd N , respectively.

REFERENCES

- [1] Y. Lin, "Editorial: First quarter 2019 IEEE communications surveys and tutorials," *IEEE Commun. Surveys Tuts.*, vol. 21, no. 1, pp. 1–9, Firstquarter 2019.
- [2] C.-X. Wang, F. Haider, X. Gao, X.-H. You, Y. Yang, D. Yuan, H. Aggoune, H. Haas, S. Fletcher, and E. Hepsaydir, "Cellular architecture and key technologies for 5G wireless communication networks," *IEEE Commun. Mag.*, vol. 52, no. 2, pp. 122–130, Feb. 2014.
- [3] J. N. Laneman, D. N. C. Tse, and G. W. Wornell, "Cooperative diversity in wireless networks: Efficient protocols and outage behavior," *IEEE Trans. Inf. Theory*, vol. 50, no. 12, pp. 3062–3080, Dec. 2004.
- [4] J. N. Laneman and G. W. Wornell, "Distributed space-time-coded protocols for exploiting cooperative diversity in wireless networks," *IEEE Trans. Inf. Theory*, vol. 49, no. 10, pp. 2415–2425, Oct. 2003.
- [5] D. K. P. Asiedu, H. Lee, and K. Lee, "Simultaneous wireless information and power transfer for decode-and-forward multihop relay systems in energy-constrained IoT networks," *IEEE Internet Things J.*, vol. 6, no. 6, pp. 9413–9426, Dec. 2019.
- [6] Y. Zou, J. Zhu, and X. Jiang, "Joint power splitting and relay selection in energy-harvesting communications for IoT networks," *IEEE Internet Things J.*, vol. 7, no. 1, pp. 584–597, Jan. 2020.
- [7] Y. Chen, N. Zhao, Z. Ding, and M. Alouini, "Multiple UAVs as relays: Multi-hop single link versus multiple dual-hop links," *IEEE Trans. on Wireless Commun.*, vol. 17, no. 9, pp. 6348–6359, Sep. 2018.
- [8] D. N. K. Jayakody, T. D. P. Perera, A. Ghrayeb, and M. O. Hasna, "Self-energized UAV-assisted scheme for cooperative wireless relay networks," *IEEE Trans. on Veh. Technol.*, vol. 69, no. 1, pp. 578–592, Jan. 2020.
- [9] Y. Lou, Q.-Y. Yu, J. Cheng, and H.-L. Zhao, "Exact BER analysis of selection combining for differential SWIPT relaying systems," *IEEE Signal Process. Lett.*, vol. 24, no. 8, pp. 1198–1202, May 2017.
- [10] P. Liu, S. Gazor, I.-M. Kim, and D. I. Kim, "Energy harvesting noncoherent cooperative communications," *IEEE Trans. Wireless Commun.*, vol. 14, no. 12, pp. 6722–6737, July 2015.
- [11] M. A. Hossain, R. Md Noor, K. A. Yau, I. Ahmedy, and S. S. Anjum, "A survey on simultaneous wireless information and power transfer with cooperative relay and future challenges," *IEEE Access*, vol. 7, pp. 19 166–19 198, Jan. 2019.
- [12] X. Chen, D. W. K. Ng, W. Yu, E. G. Larsson, N. Al-Dhahir, and R. Schober, "Massive access for 5G and beyond," *arXiv preprint arXiv:2002.03491*, Feb. 2020.
- [13] J. N. Laneman, D. N. C. Tse, and G. W. Wornell, "Cooperative diversity in wireless networks: Efficient protocols and outage behavior," *IEEE Trans. Inf. Theory*, vol. 50, no. 12, pp. 3062–3080, Dec. 2004.
- [14] T. Wang, A. Cano, G. B. Giannakis, and J. N. Laneman, "High-performance cooperative demodulation with decode-and-forward relays," *IEEE Trans. Commun.*, vol. 55, no. 7, pp. 1427–1438, July 2007.
- [15] M. R. Bhatnagar and A. Hjørungnes, "ML decoder for decode-and-forward based cooperative communication system," *IEEE Trans. Wireless Commun.*, vol. 10, no. 12, pp. 4080–4090, Oct. 2011.

- [16] H. Kim, T. Kim, M. Min, and G. Im, "Low-complexity detection scheme for cooperative MIMO systems with decode-and-forward relays," *IEEE Trans. Commun.*, vol. 63, no. 1, pp. 94–106, Jan. 2015.
- [17] X. Wang, B. Qian, and W. H. Mow, "Near-maximum-likelihood decoding for convolutionally coded physical-layer network coding over the full-duplex two-way relay channel," *IEEE Trans. Veh. Technol.*, vol. 67, no. 9, pp. 8944–8948, Sep. 2018.
- [18] Y. Lu and W. H. Mow, "Low-complexity detection and performance analysis for decode-and-forward relay networks," in *ICASSP 2019 - 2019 IEEE International Conference on Acoustics, Speech and Signal Processing (ICASSP)*, May 2019, pp. 4819–4823.
- [19] T. Himsoon, W. Su, and K. J. R. Liu, "Differential modulation for multi-node amplify-and-forward wireless relay networks," in *IEEE Wireless Communications and Networking Conference, 2006. WCNC 2006.*, vol. 2, April 2006, pp. 1195–1200.
- [20] W. Guan and K. R. Liu, "Performance analysis of two-way relaying with non-coherent differential modulation," *IEEE Trans. Wireless Commun.*, vol. 10, no. 6, pp. 2004–2014, June 2011.
- [21] M. R. Bhatnagar and O. Tirkkonen, "PL decoding in double differential modulation based decode-and-forward cooperative system," *IEEE Commun. Lett.*, vol. 17, no. 5, pp. 860–863, April 2013.
- [22] L. Lo, W. Huang, R. Y. Chang, and W. Chung, "Noncoherent detection of misbehaving relays in decode-and-forward cooperative networks," *IEEE Commun. Lett.*, vol. 19, no. 9, pp. 1536–1539, Sep. 2015.
- [23] P. Liu, S. Gazor, I.-M. Kim, and D. I. Kim, "Energy harvesting noncoherent cooperative communications," *IEEE Trans. Wireless Commun.*, vol. 14, no. 12, pp. 6722–6737, July 2015.
- [24] L. Mohjazi, S. Muhaidat, and M. Dianati, "Performance analysis of differential modulation in SWIPT cooperative networks," *IEEE Signal Process. Lett.*, vol. 23, no. 5, pp. 620–624, May 2016.
- [25] Deqiang Chen and J. N. Laneman, "Modulation and demodulation for cooperative diversity in wireless systems," *IEEE Trans. Wireless Commun.*, vol. 5, no. 7, pp. 1785–1794, July 2006.
- [26] Z. Fang, L. Li, X. Bao, and Z. Wang, "Generalized differential modulation for amplify-and-forward wireless relay networks," *IEEE Trans. Veh. Technol.*, vol. 58, no. 6, pp. 3058–3062, Jan. 2009.
- [27] Z. Fang, F. Liang, L. Li, and L. Jin, "Performance analysis and power allocation for two-way amplify-and-forward relaying with generalized differential modulation," *IEEE Trans. Veh. Technol.*, vol. 63, no. 2, pp. 937–942, Sep. 2014.
- [28] K. Kadathlal, H. Xu, and N. Pillay, "Generalised differential scheme for spatial modulation systems," *IET Communications*, vol. 11, no. 13, pp. 2020–2026, 2017.
- [29] Y. Zhu, P.-Y. Kam, and Y. Xin, "Differential modulation for decode-and-forward multiple relay systems," *IEEE Trans. Commun.*, vol. 58, no. 1, Jan. 2010.
- [30] M. R. Bhatnagar, "Decode-and-forward-based differential modulation for cooperative communication system with unitary and nonunitary constellations," *IEEE Trans. Veh. Technol.*, vol. 61, no. 1, pp. 152–165, Nov. 2012.
- [31] B. Qian and W. H. Mow, "A near BER-optimal decoding algorithm for convolutionally coded relay channels with the decode-and-forward protocol," *IEEE Trans. Wireless Commun.*, vol. 16, no. 3, pp. 1767–1781, Mar. 2017.
- [32] M. Abramowitz and I. Stegun, *Handbook of Mathematical Functions*. AAPT, 1966, vol. 34, no. 2.
- [33] E. Morgado, I. Mora-Jimenez, J. J. Vinagre, J. Ramos, and A. J. Caamano, "End-to-end average BER in multihop wireless networks over fading channels," *IEEE Trans. Wireless Commun.*, vol. 9, no. 8, pp. 2478–2487, Aug. 2010.
- [34] M. K. Simon and M.-S. Alouini, *Digital Communication over Fading Channels*. John Wiley & Sons, 2005, vol. 95.
- [35] I. S. Gradshteyn and I. M. Ryzhik, *Table of Integrals, Series, and Products*. Academic press, 2014.